UNIVERSIDADE D
COIMBRA

Diana Filipa Coutinho Santos

EPICARDIAL ADIPOSE TISSUE BIOLOGY

Dissertação no âmbito do Mestrado em Biologia Celular e Molecular orientada pela Doutora Eugénia Maria Lourenço Carvalho e apresentada ao Departamento das Ciências da Vida.

Agosto de 2018

EPICARDIAL ADIPOSE TISSUE BIOLOGY

Diana Filipa Coutinho Santos

Dissertação de mestrado no âmbito do Mestrado em Biologia Celular e Molecular orientada pela Doutora Eugénia Maria Lourenço Carvalho e co-orientada pelo Professor Doutor Carlos Manuel Marques Palmeira e apresentada ao Departamento das Ciências da Vida

Agosto de 2018

UNIVERSIDADE D
COIMBRA

This Master thesis project entitled:" Epicardial adipose tissue biology", was performed in Obesity, Diabetes and complications group, ate the Center for Neuroscience and Cell Biology, University of Coimbra, under scientific guidance of Doctor Eugénia Carvalho,

CNC
CENTER FOR NEUROSCIENCE AND CELL BIOLOGY
UNIVERSITY OF COIMBRA, PORTUGAL

And would not have been possible without the funding by:

FEDER support by *Programa Operacional Factores de Competetividade – Compete 2020*, national support by *FCT – Fundação para a Ciência e Tecnologia through the strategic project* COMPETE: POCI-01-0145-FEDER-007440, and by the Portuguese Transplantation Society (SPT), Portuguese Diabetes Society (SPD), European Foundation for the Study of Diabetes (EFSD), as well as HealthyAging2020: CENTRO-01-0145-FEDER-000012N2323.

EFSD
European Foundation for the Study of Diabetes

SOCIEDADE PORTUGUESA DIABETOLOGIA
PORTUGUESE SOCIETY OF DIABETOLOGY

SPT
Sociedade Portuguesa de Transplantação

AGING HEALTHY 2020

FCT Fundação para a Ciência e a Tecnologia
MINISTÉRIO DA CIÊNCIA, TECNOLOGIA E ENSINO SUPERIOR

COMPETE
PROGRAMA OPERACIONAL FACTORES DE COMPETITIVIDADE

QREN
QUADRO DE REFERÊNCIA ESTRATÉGICO NACIONAL
PORTUGAL 2007.2013

UNIÃO EUROPEIA
Fundo Europeu de Desenvolvimento Regional

Agradecimentos

Chegou o fim de mais uma etapa e não poderia deixar de agradecer a todas as pessoas que me apoiaram:

Em primeiro lugar gostaria de agradecer à Doutora Eugénia Carvalho pela oportunidade única de desenvolver esta tese de mestrado no seu laboratório, por aceitar ser minha orientadora, por toda a paciência, confiança e disponibilidade que mesmo do outro lado do oceano sempre mostrou.

Ao Doutor Carlos Palmeira, pela co-orintação.

Ao Professor Doutor Manuel Antunes e a toda a sua equipa do centro de cirurgia cardiotorácica, pela ajuda fundamental na disponibilização das amostras humanas usadas neste estudo, mas também pela forma calorosa como sempre me acolheram.

À Doutora Ana Catarina Fonseca, por supervisionar o meu trabalho experimental, pela confiança e ajuda e ainda por ser sempre incansável ao responder a todas as minhas dúvidas, desesperos e desvaneios.

À Doutora Ana Burgeiro, pelo fundamental apoio nesta fase final de interpretação de resultados e de escrita.

Agradeço sinceramente a todos os meus colegas do grupo: “Obesity, Diabetes and complications”, cada um de vocês contribui de uma forma particular para a realização deste trabalho. Um agradecimento especial à Aryane, pela tão preciosa ajuda na recolha das amostras e no demais trabalho laboratorial. Marija, Giada e Raphael, muito obrigada pelo esforço na compreensão do meu inglês, na confiança e no carinho que sempre demonstraram para comigo, #itsnervermyfault.

Agradeço também ao Nuno, por toda ajuda na parte estatística.

Um grande obrigado a todos os meus amigos, à Eduarda, Márcia, Rita, Andreia, Ana Figueiredo, Ana Gomes, Cristiana, Marta, Laura, Rafael, Beatriz, ao Roberto, Maria e Carolina e ainda aos amigos dos Escuteiros e aos do restaurante, por todo o carinho, compreensão e apoio que demostraram desde o momento em que vos conheci. Um

agradecimento especial à Catarina, que após 2 universidades e um estágio em *Erasmus* ainda consegue ter paciência para me aturar.

Ao Tiago, o namorado que me acompanha desde ainda antes da minha aventura académica começar, por toda a amizade, carinho, amor, compreensão e paciência...muita paciência, por ser o meu maior apoiante e o mais entusiasta, sempre na primeira fila pronto a festejar cada vitória minha como se do Benfica se tratasse.

Por fim, um agradecimento muito especial aos meus pais, Carla e Valdemar e ao meu irmão Márcio, por todo o apoio ao longo dos anos, por me ensinarem que nada se alcança sem trabalho, a ser humilde e responsável. Não podia deixar também de agradecer à Linda por todo o apoio nestes últimos meses e à companheira de 4 patas, a Star.

Todos os que foram referidos ao longo deste texto ocupam um lugar muito especial no meu coração e contribuíram de alguma forma para a realização deste trabalho,

A todos um sincero Obrigado.

Abstract

Until recently, adipose tissue was thought to be only a fat storage organ, only in the last decades studies have shown that it is more than just a fat storage depot. Epicardial adipose tissue (EAT) is a specific fat depot that involves almost 80% of the heart. It is responsible for the secretion of a variety of bioactive molecules that can regulate metabolic and immune functions, with protective effect to cardiomyocytes and coronary arteries. EAT has high plasticity, its thickness undergoes a constant volume adaptation and consequently alteration in adipocyte number and size, in response to aging, diet, drugs and pathologies, such as diabetes. Metabolic alterations in fat may affect several metabolic pathways, such as fatty acid (FA) oxidation and cardiac metabolism by modulating FA uptake and insulin action. Despite the important physiological role of EAT in cardiovascular metabolism, few studies have been carried out in order to evaluate its therapeutic potential.

The aim of this study was the characterization of EAT, regarding the expression of some proteins related with insulin signaling, as well as mitochondrial respiration, in comparison to subcutaneous adipose tissue (SAT). The results presented are only preliminary due the small number of samples obtained to date, more tissues will need to be studied for a solid and robust conclusion.

Results from a manuscript in preparation from our group, show increased mitochondrial respiration in EAT when compared to SAT, when supplied substrates that fuel NADH-linked oxidative phosphorylation (OXPHOS). Moreover, the differences observed were annulled after UCP1 inhibition with GDP, under these conditions. Thus, a specific protocol for evaluation of FA-contribution to OXPHOS was used in EAT and SAT from HF patients. In the present study we shown an increased mitochondrial respiration in EAT due to the contribution of the FA oxidation, in spite of UCP1 inhibition, when compared to SAT. These results emphasize EAT's role in lipid metabolism, and a primary source of substrates to the nearby, always working cardiomyocyte. Due the anatomical relation and proximity between EAT and the heart, the metabolic characterization of EAT might contribute to the discovery of early biomarkers for potential therapeutic targets, in cardiac disease.

Key Words: Epicardial adipose tissue, Heart failure, Insulin signaling, Mitochondrial respiration, Fatty acid oxidation.

Resumo

Apenas nas últimas décadas os estudos mostraram que o tecido adipose era mais do que um órgão capaz de armazenar gordura, como era considerado até então. O tecido adiposo epicardial (TAE) e um tipo específico de gordura que envolve cerca de 80% do coração. Em condições fisiológicas normais, TAE é responsável pela secreção de várias biomoléculas que exercem um efeito protetivo nos cardiomiócitos e artérias coronárias, uma vez que é capaz de regular tanto funções metabólicas como imunes. O TAE apresenta uma elevada plasticidade, alterações no número e tamanho dos adipócitos promovem uma constante adaptação do volume, como resposta à idade, dieta, drogas e patologias como a diabetes. As alterações metabólicas nas células gordas podem afetar várias vias metabólicas, incluindo a oxidação dos ácidos gordos e metabolismo cardíaco através da modulação do *uptake* dos ácidos gordos, sinalização da insulina e *uptake* da glucose em resposta à insulina. Apesar do importante papel fisiológico do TAE no metabolismo cardiovascular, apenas alguns foram desenvolvidos de forma a avaliar o seu potencial terapêutico. O objetivo deste estudo, consiste na caracterização do TAE, tendo em conta a expressão de proteínas relacionas com a sinalização da insula e a respiração mitocondrial em comparação com o tecido adiposo subcutâneo (TAS). Contudo, os resultados apresentados tendo em conta a expressão das proteínas envolvidas na sinalização da insulina, são apenas preliminares uma vez que o número de amostras envolvidas é muito reduzido e consequentemente mais tecidos necessitam de ser comparados de forma a obter resultados mais robustos e conclusivos.

Resultados provenientes de um manuscrito em preparação do nosso grupo, mostraram um aumento da respiração mitocondrial no TAE em comparação com o TAS. Os resultados mostram ainda que as diferenças observadas entre os tecidos são anulados após inibição da UCP1. Deste modo, um novo protocolo foi usado de forma a avaliar a contribuição da oxidação dos ácidos gordos na fosforilação oxidativa tanto no TAE como no TAS de doentes com falha cardíaca. No presente estudo, mostramos um aumento na respiração mitocondrial com a contribuição da oxidação dos ácidos gordos no TAE quando comparado com o TAS, quando a UCP1 está inibida. Estes resultados enfatizam a contribuição do TAE na manutenção dos elevados requerimentos energéticos do cardiomiócitos, devido á sua constante função contráctil. A caracterização de TAE, pode

contribuir para a descoberta de bio marcadores que podem funcionar como potenciais alvos terapêuticos na doença cardíaca.

Palavras-chave: Tecido adiposo epicardial, Insuficiência cardíaca, Sinalização da insulina, Respiração mitocondrial, oxidação dos ácidos gordos.

List of abbreviations

AA – Antimycin A

ADP – Adenosine diphosphate

AKT – Serine/Threonine Kinase 1

AKT/PKB – Protein kinase B

ALT – Alkaline phosphatase

AMPK – Adenosine monophosphate (AMP)-activated protein kinase

AT – Adipose tissue

ATP – Adenosine triphosphate

Asc– Ascorbate

BAT – Brown adipose tissue

BCA - Bicinchoninic acid

BMI c Body mass index

BSA – Bovine serum albumin

C/EBP – CCAAT/enhancer-bind protein

Ca^{2+} – Calcium ion

CAD – Coronary artery disease

CCCP – Carbonyl Cyanide 3-chlorophenyl hydrazone

CREB – cAMP-responsive element binding protein

CVD – Cardiovascular disease

CK – Creatine kinase

Cyt c – Cytochrome c

DAG – Diacylglycerol

DPP4 – Dipeptidyl peptidase-4

DM – Diabetes Mellitus

EAT – Epicardial adipose tissue

ECL – enhanced chemiluminescence

ECM – Extracellular matrix

ERK – Extracellular signal-regulated kinase

ET – Electron transfer

FA – Fatty acid

$FADH_2$ – Flavin adenine dinucleotide

FABP – Fatty acid binding proteins

FAS – Fatty acid synthase

FCCP – Trifluoromethoxy carbonylcyanide phenylhydrazone

FFA – Free fatty acids

F-pathway – FA oxidation

GDP – Guanosine diphosphate

GLP1/2 – Glucagon like peptide 1/2

GLUT4 – Glucose transporter 4

GTP – Glutamic pyruvic transaminase

GOP – gamma glutamyl transferase

HDL – High density lipids

HEPES – 4-(2-hydroxyethyl)-1-piperazineethanesulfonic acid

HF – Heart failure

HRP – Horseradish peroxidase

HRR – High resolution respirometry

ICM – Ischemic cardiomyopathy

IDF – International Diabetes Federation

IL-6 – Interleukin 6

IR – Insulin receptor

IRS1 – Insulin receptor substrate 1

JNK – c-Jun N-terminal kinases

KHR – Krebs-Ringer HEPES

Mal – Malate

MAPK – Mitogen activated protein kinase

MDCT – Multidetector computed tomography

MPC-1 – Monocyte chemotactic protein

N-pathway – NADPH pathway

NADH – Nicotinamide adenine dinucleotide

NADPH – Nicotinamide adenine dinucleotide phosphate

NCAD – Non-coronary artery disease

NDM – Non-DM

NO – Nitric oxide

NODAT – New onset diabetes after transplantation

NOS – Nitrogen oxygen species

O^{2-} – Superoxide anion

Oct – Octanoylcarnitine

Omy – Oligomycin

OXPHOS – Oxidative phosphorylation

PAD – Peripheral Vascular Disease

PI3K – Phosphoinositide 3-Kinase

PGC1α – Peroxisome proliferator-activated receptor gamma coactivator 1-alpha

PMG – Pyruvate, Malate and Glutamate

PPARγ – Peroxisome proliferator activated receptor gamma

PVDF – polyvinylidene fluoride

RAS – Renin-angiotensin system

ROS – Reactive oxygen species

ROX – Residual oxygen consumption

ROT – Rotenone

SAT – Subcutaneous adipose tissue

SDS-PAGE – Sodium dodecyl sulfate polyacrylamide gel electrophoresis (

SREBP – Sterol regulatory element binding proteins

SUIT – Substrate-uncoupler-inhibitor titration

Succ – Succinate

T1DM – Type 1 diabetes mellitus

T2DM – Type 2 diabetes mellitus

TCA cycle – Tricarboxylix acid

TG – Triglycerides

TGF β – Transforming growth factor beta

TMED - N´, N´, N´, N´ tetramethyllethylenediamine

TNF α – Tumor necrosis factor α

TMPD – Tetramehyl-p-phenylenediamine

UCP – Uncoupling protein

VAT – Visceral adipose tissue

WAT – White adipose tissue

WB – Western blot

Table of Contents

LIST OF FIGURES

LIST OF TABLES

Chapter 1. Introduction

1.1 Diabetes Mellitus

Epidemiology

Diabetes Mellitus (DM) is one of the 21st century epidemies, and a severe global health problem. It represents a group of several metabolic disorders that share the increased levels of blood glucose as risk factor (1).

Data from the International Diabetes Federation (IDF) shows that almost all countries around the world are affected by this pathology. Since the first study in 1985, where about 30 million diabetic cases were estimated, this number has increased almost 14 times, to 415 million diabetic patients in the last report from 2015 and the tendency is for diabetes to increase its incidence. It is expected to reach 642 million affected people in 2040 (Figure 1) (2).

Figure 1. Prevalence and incidence of adults (20-79 years) with diabetes in 2015, and the estimated number for diabetic incidence in 2040, per region. Adapted from IDF, 2015 (2).

In Portugal, the number of diabetic patients is also increasing. Nowadays more than 13% of the adult population (20 – 79 years) is diabetic (3). This number is associated with the ageing of the population, and the increasing numbers of overweigh and obese individuals, as a consequence of environmental factors, including high calorie food intake and lower or non-existent physical activity (3).

Globally an estimated 5 million diabetic individuals die from the disease annually, pointing to diabetes as the third most common cause of death worldwide (2). Moreover, it represents a massive socio-economic burden, with about 12% of the global health care expenditure and 10% in Portugal (2,3).

Characterization

Diabetes can be divided in several subgroups, regarding the development of the disease (1). The major types of diabetes are Type 1 diabetes mellitus (T1DM), affecting about 10% of the diabetics, while Type 2 (T2DM) accounts for about 90% of the diabetes cases (2). The other subgroups of diabetic individuals with lowest incidence are a result of specific gene mutations, or diseases that alter insulin function or sensitivity. One of these less but most warning subgroups is gestational diabetes, that is a high-risk factor for the mother and child to develop diabetes later in life. Figure 2 shows these three major diabetes subtypes and the correspondent etiology (2).

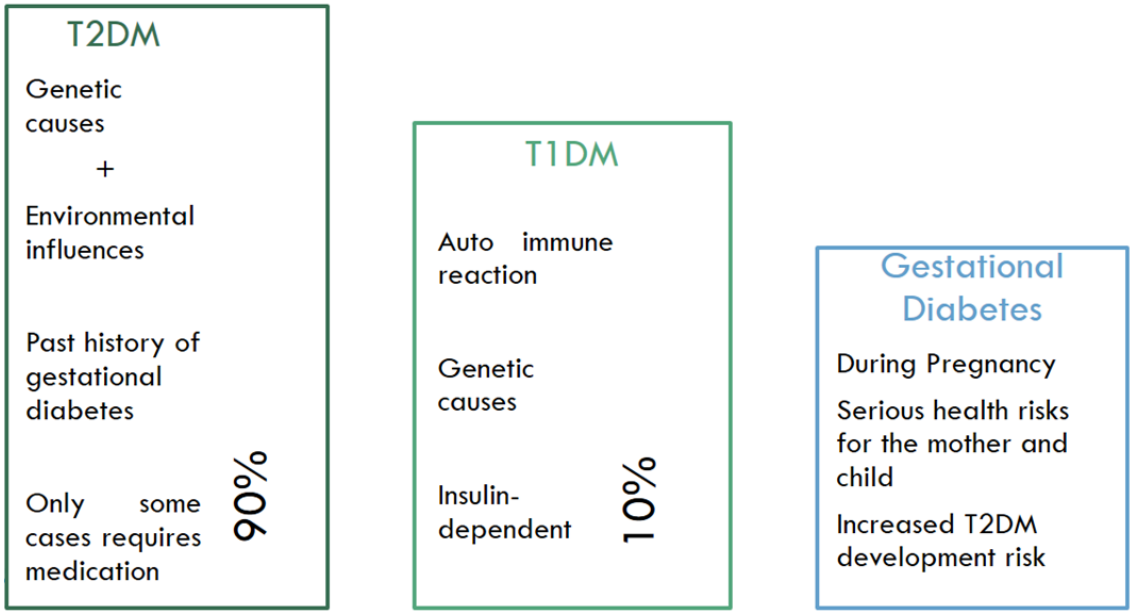

Figure 2. Different subgroups of diabetes Mellitus.

T1DM is the result of an autoimmune reaction, where pancreatic β-cells are destroyed by immune cells, leading to an inflammatory reaction (4). The major cause is the genetic predisposition conjugated with environmental factors, as virus or chemical compounds (4,5). Once these insulin-producing cells are affected, there is a significant reduction in insulin secretion, insufficient to maintain whole blood glucose homeostasis.

As a result, all T1DM patients are insulin-dependent. It normally affects people early in life, therefore a person with T1DM will live suffering from the disease their entire life.

On the other hand, in T2DM, the pancreatic β-cells may be normal, even if the insulin levels are altered in some cases. What happens in these individuals is a decrease in insulin sensitivity, and insulin action, promoting insulin resistance (6). Insulin resistance occurs despite normal, and, sometimes, increased, insulin secretion by pancreatic β-cells, there are deficient responses to the insulin stimuli at the cellular level (7). Insulin action, including insulin signaling and glucose uptake into insulin sensitive tissues can become compromised in subjects with insulin resistance (Figure 3), as is the case not only in T2DM subjects but also in about 30% of their first-degree relatives (8–11).

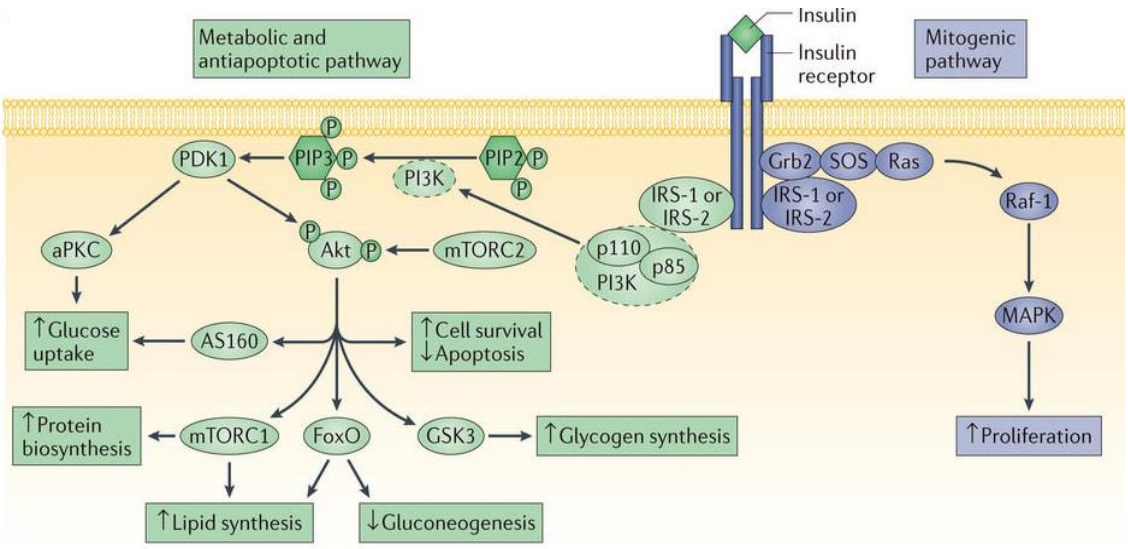

Figure 3. The insulin signaling pathway. Insulin is an anabolic hormone that binds to the insulin receptor and promotes the recruitment of insulin receptor substrate (IRS) isoforms and subsequent activation of the phosphatidylinositol 3-kinase (PI3K)-Protein Kinase B (PKB/AKT), which promotes regulation of glucose and lipid metabolism, protein biosynthesis, cell survival and apoptosis. Insulin can lead to increased cell proliferation by activation of the mitogen-activated protein kinase (MAPK) pathway. Adapted from (12).

As shown in the Figure 2, there are environmental factors that increase the risk to develop T2DM. Obesity, another 21st century epidemy, occurs when a diet rich in calories and fat is conjugated with low or inexistent physical activity, leading to a significant increase in body fat and weight. As a consequence of obesity, some people develop insulin resistance, and consequent alteration in blood glucose levels – hyperglycemia (6,13). Higher glucose levels present in the blood can induce glucose intolerance. Insulin resistance "blocks" the entrance of glucose into tissues and a

compensatory effect occurs increasing the hepatic glucose production, by gluconeogenesis, intensifying the hyperglycemia (14).

Diabetes complications

Alterations in glucose homeostasis as a result of long-term impaired glucose regulation and insulin resistance, can lead to other metabolic alterations, such as hypertension and dyslipidemia (hypertriglyceridemia and low high-density lipoproteins (HDL) cholesterol levels). These alterations represent a cluster of clinical disorders, and when they are associated with obesity or simply with an increase in abdominal adiposity, can lead to the metabolic syndrome (15).

Additionally, diabetes increases the risk for micro and macrovascular alterations that lead to diabetes complications (16). At the microvascular level, the diabetes complications include diabetic retinopathy, nephropathy and neuropathy, as a consequence of the dysregulation in the blood glucose levels, Figure 4 (17–19).

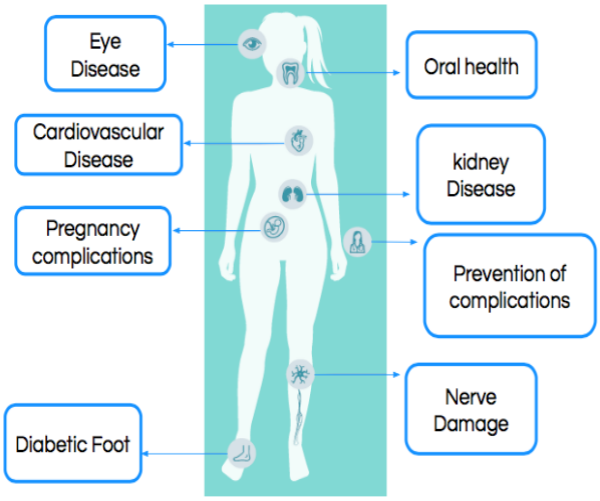

Figure 4. Macrovascular complications of diabetes (2).

However, when macrovascular alteration and chronic inflammation are present it can lead to atherosclerosis (16,20). Cardiovascular Diseases (CVD) can be a consequence of these alterations, affecting the heart and the coronary vessels, as well as the circulatory system, leading to several alterations in peripheral and neuronal blood supply (16).

Most complications associated with diabetes can be prevented or delayed by the proper regulation of the important risk factors such as blood glucose levels, blood pressure and cholesterol levels, however, these complications can be lethal if not treated properly (21).

1.2 Cardiovascular Disease

One of the most lethal complication of diabetes is cardiovascular disease, and it is present in subjects with T1DM, as well in T2DM (21,22). Diabetes is considered a major risk factor for the development of CVD (16). Low levels of physical activity promote the accumulation of abdominal fat that is associated with impaired glucose regulation, insulin resistance, dyslipidemia and hypertension. Together, they can promote alterations in inflammation, coagulation capacity (hypercoagulation) and consequently formation of atherosclerotic plaques (2,16,21,23,24).

There are three major types of CVD subgroups, depending on which vessel is affected and, as a consequence, which body regions that is affected, namely Stroke, Peripheral Vascular Disease and Coronary artery disease (CAD) (Figure 5). A stroke occurs when the vessels affected are responsible to supply blood to the brain. When these vessels are blocked or ruptured, less blood reaches the brain and, depending on the brain region that is affected, several types of consequences can occur. Cerebral infarction and cerebral hemorrhage are the most common features than can trigger a stroke (25). When the vessels affected are responsible to supply blood to a lower member, Peripheral Vascular Disease (PAD) is developed. In this way, a lower blood flux can reach to the legs and feet. In the most severe cases, the death of the tissue can occur, or gangrene, a disease state most prevalent in diabetic individuals (26).

Besides, we are presented with CAD if the coronary vessels are affected. CAD includes several heart diseases as heart attack, myocardial infarction and coronary heart disease (27). Very recently studies have shown that oscillations in glucose levels as a response of dysfunction in the pancreatic β- cells, can be enough to develop CAD, even in patients with normal glucose tolerance (28). All these alterations occur because the heart does not receive the normal blood supplies (2,16,20,21,29).

Very recently studies have shown that oscillations in glucose levels as a response of dysfunction in the pancreatic β-cells, can be enough to develop CAD, even in patients with normal glucose tolerance (28).

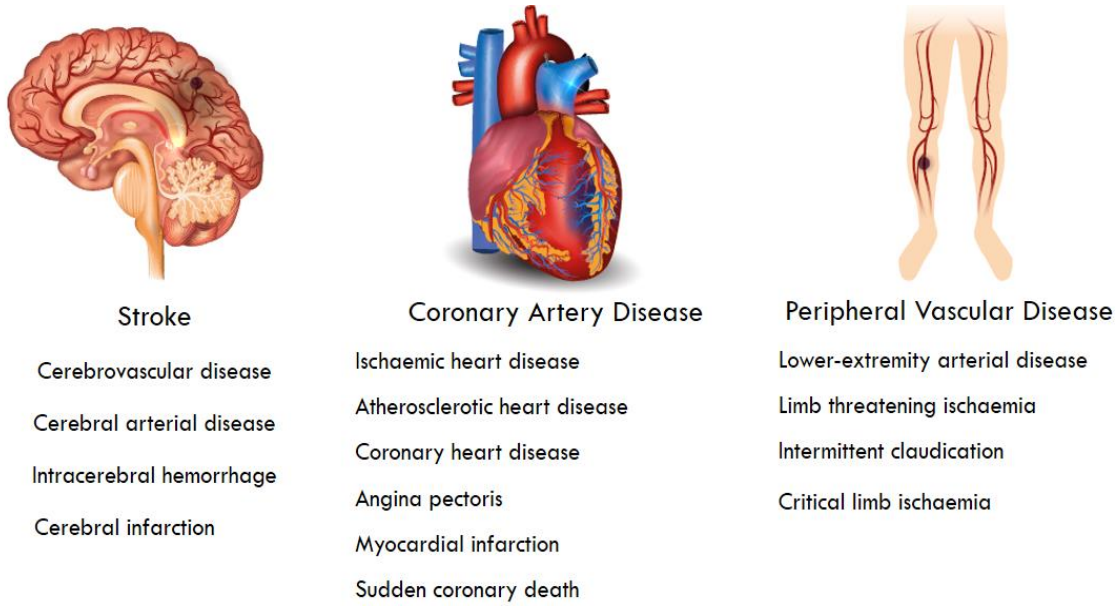

Figure 5. Three major types of CVD. Adapted from (2,29).

1.3 Adipose Tissue

Adipose tissue (AT) has been associated with several metabolic and physical alterations that are present in diabetes, and consequently with CVD. Several factors that include increased body weight, pancreatic β-cell dysfunction, insulin resistance and glucose intolerance are largely associated with alterations that occur in AT during the obesity process (30).

Some T2DM patients present normal body mass index (BMI). In these patients, T2DM arises as a result of diminished insulin secretion more than insulin resistance, even though they are not considered obese, these patients present higher levels of adiposity (31). On the other hand, not all obese individuals are diabetic; some of them can be considered metabolically healthy, with the typical obese metabolic features absent (32).

Adipose Tissue Physiology

AT is the tissue with most plasticity, it is widely distributed in the body and may represent more than 20% of the adult body weight. A specific AT location is associated with a specific function (33,34).

There are several cell types present in AT, including adipocytes, immune cells, fibroblasts, cells from the vascular and nervous systems and pre-adipocytes, which latter can be differentiated into mature adipocytes (33,34). In addition, there are several bioactive molecules that are secreted by AT – adipocytokines. The production and secretion of these bioactive molecules are actively related with the fat mass and they modulate inflammation, as well as lipid and glucose metabolism (35–37). In this way, AT contributes to the maintenance of systemic energy balance (38).

There are three types of mature adipocytes: white, brown and beige (Figure 6) (39). They are present in the two, brown adipose tissue (BAT) and white adipose tissue (WAT) major types of AT of mammals (39). Apart from the distinct color, BAT and WAT can also be considered tissues with antagonistic functions (40).

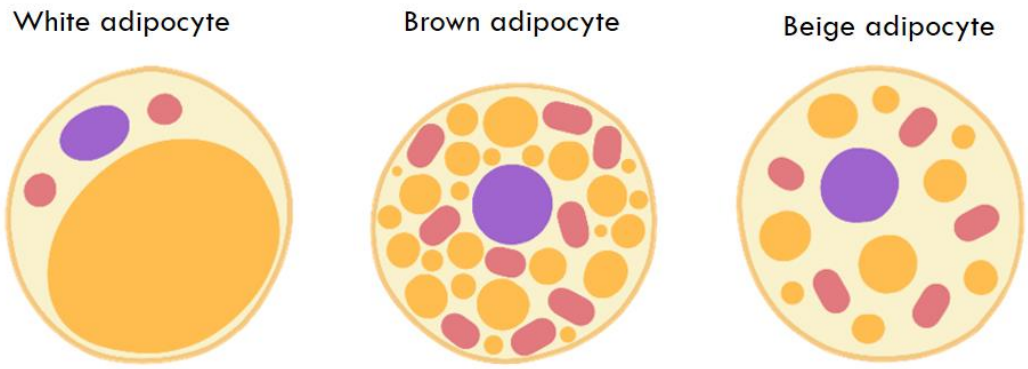

Figure 6. Representations of the three types of adipocytes. White adipocytes are typically spherical, filled by a single and large lipid droplet, with little cytoplasm and few mitochondria. Brown adipose cells present smaller dimensions, with large numbers of mitochondria and multiple lipid droplets. Beige adipocytes exhibit mixed characteristics. Purple: nucleus; red: mitochondria; yellow: lipid droplets. Adapted from (41).

BAT has high thermogenic capacity, which means high capacity to convert chemical energy obtained from food into dissipated energy in the form of heat (42). It is mainly present in newborns and it is significantly decreased in adults, but it is still related with a diversity of metabolic alterations and energy homeostasis, since its main characteristic is the increased number of mitochondria (40). The function of beige adipocytes may overlap with brown and white adipocytes; they are a specific type of

cells with a unique transcriptome, also associated with the thermogenic capacity, as well as white adipocytes phenotypes, such as large lipid droplets (42). However, when the environmental conditions are altered, and the temperature decreases, the beige adipocyte number increases due to WAT "browning", and an increase in the expression of brown adipocytes related features/markers, including increased expression of the uncoupling protein-1 (UCP1) (39,42,43).

WAT is the AT most abundant in adults. It is specialized in the storage of excess of energy in the form of triglycerides (TG) and Free Fatty Acids (FFA), which can be released during fasting, starvation, or exercise periods, preventing lipotoxicity in other tissues (43). However, in the last few years, WAT was also been described as an endocrine organ, capable of secreting several adipocytokines directly in the circulatory system and consequently regulating distant organs (37).

WAT is divided into subcutaneous adipose tissue (SAT) and visceral adipose tissue (VAT). SAT is present in the subcutaneous layers under the skin throughout the body and can be subdivided into abdominal, femoral and gluteal, according to the correspondent location (39).VAT surrounds the major organs but can include some SAT, and, depending on the specific location, it can also be subdivided in epicardial, gonadal, mesenteric, omental and retroperitoneal (39).

White Adipose Tissue -healthy and unhealthy conditions

Under normal conditions, white adipocytes are responsible to generate TG, via lipogenesis by esterification of glycerol 3-phosphate and acetyl-CoA, for posterior release during lipolysis (44).

WAT is an endocrine organ that can modulate metabolism of other tissues, through the secretion of several molecules, as leptin, adiponectin, resistin, FFA, as well as other proteins that are involved in inflammation, for example: pro-inflammatory cytokines, tumor necrosis factor-alpha (TNF-α), interleukin 6 (IL-6) and monocyte chemotactic protein -1 (MCP-1) (13,44).

These bioactive molecules are easily diffused through the whole body, due to the high vascularization that accompanies the adipose tissue niche, and promote the

communication with other cells, tissues and organs (37). The extended vascularization supplies oxygen, nutrients, growth factors, hormones and cytokines, requirements to maintain normal AT function (37,43,45).

Secretion of some of these adipocytokines is responsible for the modulation of blood glucose homeostasis. In general, some of these molecules, such as leptin and adiponectin, can exert anti-hyperglycemic action by the activation of adenosine monophosphate (AMP)-activated protein kinase (AMPK) and peroxisome proliferator activated receptor (PPAR)-γ that promote the increase in FA oxidation and insulin sensitivity (46,47). On the other hand, resistin can exert hyperglycemic action in tissues, leading to negative effects in insulin action (48). The release of pro-inflammatory cytokines, such as TNF-α and IL-6 (that promote the reduction in the insulin action) is also associated with hyperglycemia (37,44,49).

Dysregulation in the WAT secretome is a key pathological phenomenon that contributes to the metabolic syndrome (44). The expansion and excess of AT as a result of overnutrition, especially in the abdominal area, is associated with adipocyte hypertrophy (33). The increased adipocyte size is largely correlated with increased inflammation and insulin resistance (33). Thus, the metabolic dysregulation occurs by the increased accumulation of FA in peripheral tissues and several organs, including liver and muscle, leading to the accumulation of several lipotoxic species, as diacylglycerol (DAG) and ceramides (50). The resultant lipotoxicity can promote insulin resistance by phosphorylation of insulin receptor 1 (IRS1) in residues that cause decreases in the activity rates from the AKT/insulin signaling pathway (33,37). Furthermore, lipotoxicity promotes the inhibition of AMPK and, consequently, decreases the levels of FA oxidation and induces insulin resistance (44,51).

In diabetic condition, as a result of the metabolic syndrome, adipocyte hypertrophy is also observed, such as all metabolic alterations referred above. Moreover, these alterations can affect several cells, tissues and organs, leading to the development of diabetes complications (13,44). In the specific case of CVD, the alterations in AT can directly modulate cardiomyocyte function and structure. However,

this modulation occurs with the interference of a specific regional fat distribution, the epicardial adipose tissue (EAT) (52).

1.4 Epicardial Adipose Tissue

Very recently, a novel type of WAT has been described, EAT, which has been associated with the development of CVD (53). EAT is located around the heart, and consequently it is considered a visceral thoracic fat, a subtype of VAT (54). Even though it represents only a small fraction of total body AT, it represents more than 20% of the total ventricular weigh and almost 15% of the total heart weigh (55).

There are other VAT depots surrounding the heart. However, EAT is the only that can communicate directly with the heart, since it is located between the visceral pericardium and myocardium, and has no *fascia layer* separating it from the underlying myocardium (56–59), Figure 7. Moreover, heart and EAT share a common embryonic origin, from the splanchnopleuric mesoderm, features that enhance the close anatomical affinity between these two organs (54).

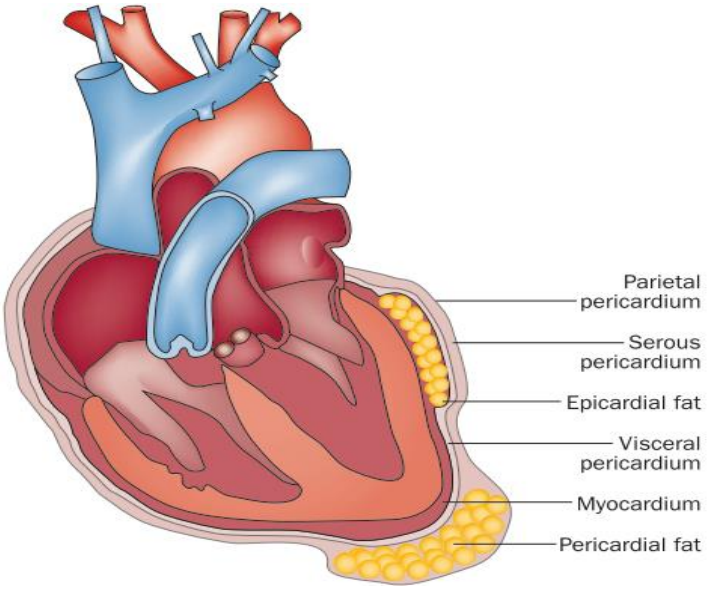

Figure 7. Localization of the heart associated VAT. Epicardial adipose tissue is located between the myocardium and visceral pericardium; pericardial adipose tissue is located outside of the visceral pericardium and on the external surface of the parietal pericardium (52).

Tiny amounts of EAT are able to penetrate connective tissue lying between the muscle bundles and muscle fibers (58). It is also usually located along the intramodal

branch of large coronary artery (52,60) and it is supplied with blood by the coronary circulation (54,61), sharing the same microcirculation of the heart (57). It has therefore been proposed that EAT is of significant importance in cardiac physiology and cardiac disease development (62).

EAT shares the same cell composition as WAT, namely, it presents white adipocytes, preadipocytes, stroma-vascular and ganglionic cells, as well as nerve and immune cells (63). Although the presence of BAT adipocytes has been studied (64). EAT is a multifaceted tissue playing a role in the mechanical, thermogenic, immune, and metabolic aspects that can affect positively or negatively cardiomyocyte function (52).

To maintain body homeostasis, the heart needs to contract and pump blood constantly, which can lead to an excessive distortion of coronary arteries. EAT presents high elasticity and, as a consequence, it is responsible to exert mechanically protection from the artery pulses and myocardial contraction (52).

Studies by Sacks et al., 2009 (65) have shown that EAT has a higher expression of genes that are normally present in BAT, when compared with other fat depots. The increased number of mitochondria expressing UCP1 and other related genes, suggests that it can protect the heart against hypothermia, through heat production (65). In fact, the transcriptome of this fat depot reveals a site-specific protein expression for EAT surrounding the coronary arteries, atria and ventricles (66).

Epicardial Adipose Tissue – a metabolic active organ

EAT, as a visceral adipocyte depot, is a metabolic active organ that is able to generate several bioactive molecules (67), that can be released by paracrine (passive diffusion through interstitial space and cellular membranes) or endocrine ways. These bioactive molecules are involved in the regulation of endothelial function, coagulation and inflammation, directly affecting the metabolic and immune functions of cardiomyocyte and coronary arteries, as well as other cells present in the same milieu (68,69).

The expression of these bioactive molecules is largely associated with the development of CVD (60,70,71). Adipokines such as adiponectin, resistin, IL-6 and IL-8, but also other markers, such as transforming growth factor-β (TFG-β), activin A,

thrombospondin 2, appear to be increased in EAT when compared with other visceral fat depots (68,70). However, it is also an abundant source of TNF-α, MCP-1, and FA binding proteins (FABP), with the expression levels correlated with several heart and coronary diseases (68,72).

In physiological conditions, adiponectin can inhibit the production of inflammatory factors (73), reduces superoxide anion (O^{2-} generation by myocardial nicotinamide adenine dinucleotide phosphate (NADPH) oxidase activity) (74) and also improve nitric oxide bioavailability and endothelial function on the coronary vasculature (63). On the other hand, it is able to activate the AMPK pathway, which can lead to an increase in FA oxidation, and reduction of lipid depots in cardiac muscle (75). In summary, adiponectin is described as having antidiabetic, antiatherogenic, antioxidant and anti-inflammatory properties (69).

Not much is known regarding the metabolic function of EAT. These adipocytes show a great capacity and flexibility for storage or release of FFA, and the enrichment of this tissue in saturated FA and its increased FA metabolism may help to provide the energy supply to the myocardium and the arterial wall by FA oxidation (76), and at the same time function as a buffer protecting the heart against FA lipotoxicity (77).

The EAT-secretome activity is regulated by systemic factors, such as metabolic condition or cardiac biology. In this case, local stimuli from the heart or the coronaries, conjugated with obese or T2DM conditions, seems to be related with the development of coronary atherosclerosis, ischemic heart failure, and arterial fibrillation (72,74).

Recent *in vitro* studies have shown that in T2DM patients the secretome released by EAT, can inhibit mitochondrial β-oxidation in primary adult rat cardiomyocytes by activation of the cardiac-specific renin-angiotensin system (RAS) by miR208 induction, after incubation with conditioned media from EAT-T2DM patients. This dysregulation occurs as a consequence of decreased mitochondrial respiration in the rat cardiomyocytes (78) .

Obese or T2DM patients may have adipocyte hypertrophy associated with tissue expansion and inflammation. This alteration promotes a switch in the normal anti-

inflammatory protector function to a pro-inflammatory state, as consequence of higher secreted levels of pro-inflammatory cytokines (68,79,80). The increased expression of activin A and decreased adiponectin expression, can negatively affect cardiac metabolism by inhibition or dysregulation of nicotinamide adenine dinucleotide (NADH) and insulin-mediated glucose uptake, and AMPK signaling (68,70,81). The local increased number of monocytes ($CD14^+$), lymphocytes ($CD3^+$), macrophages ($CD68^+$), and mast cells and their accumulation, can lead to an even greater secretion level of inflammatory adipocytokines, resulting in adipokine overactivation which is positively correlated with CAD severity (35,82,83).

Under the pathological conditions described above, an excessive FA uptake, is associated with the AT expansion, as a result of a high content in FABPs (58). Therefore, mitochondrial β-oxidation rate is increased; however, when the EAT lipid content capacity is exceed, these lipids were released and cardiomyocyte intracellular lipid content increases, contributing for the cardiomyocyte dysfunction (74).

The formation of reactive oxygen species (ROS) alters the expression of PPARγ/ adiponectin, leading to the inhibition of NADPH oxidase activity (74) and consequently increasing the lipid storage pools to the intermediate lipotoxic species, such as DAG and ceramide, that leads to mitochondrial and contractile dysfunction of cardiomyocytes (84)

In 2011 and 2012, data obtained by Greulich et al., (85,86) also showed the negative effect in sarco-/endoplasmic reticulum Ca^{2+} ATPase activity and Ca^{2+} cycling, which may promote cardiomyocyte dysfunction and it is also associated to diastolic function, myocardial fibrosis and hypertrophy in the insulin-resistant myocardium from diabetic patients (58,59).

The relationship between the EAT thickness and the development of CVD is widely accepted. However, recent studies indicate that the increased fat thickness could occur due to hyperplasia and not by a hypertrophy. An increased number of proteins of the extracellular matrix (ECM) in EAT from patients with ischemic cardiomyopathy (ICM) and cytoskeletal proteins regulated by extracellular signal regulated protein kinase 1/2

(ERK1/2) activation pathway could explain these increased fat thickness as a result of cellular proliferation (87).

Epicardial Adipose Tissue – a therapeutic target

Measurements of EAT thickness and its correlation with the development of CVD, has been possible due to the development of non-invasive imaging techniques were developed, including 64-multidetector computed tomography (64-MDCT) which is a technique largely used in cardiac pathology diagnoses. The 64-MDCT provides accurate EAT quantification when compared with other techniques, for example echocardiography or magnetic resonance (88,89), Figure 8.

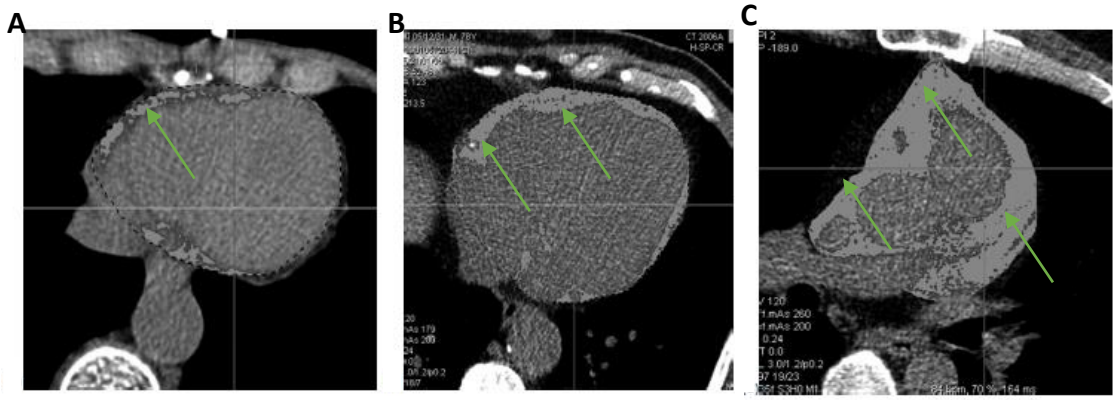

Figure 8. Representative image of EAT using Multidetector Computer Tomography. (A) Normal epicardial fat depot; **(B)** Moderately increased epicardial fat depot; **(C)** Markedly increased epicardial fat depot. Adipose tissue depots were marked with a green arrow. Adapted from (89).

Despite all the mechanisms that are related to EAT thickness and the development of several CVD, much still remains unknown. EAT as been proposed as a therapeutic target for the development of pharmaceutical agents (62).

Some of the drugs that are currently used to treat diabetes or CVD patients, as dipeptidyl peptidase-4 (DPP4) inhibitors or liraglutide, a (glucagon like peptides) GLP1 analogue, are now under analysis to try to understand how these drugs could be used to improve therapeutic strategies. In 2016, Martinez et al. (90) have shown the effect of DPP4 inhibitors in the rapid reduction of EAT thickness, by using sitagliptin (90). In addition, Iacobellis et al., (91) have recently found the expression of GLP1/2 receptors in EAT, which might explain the rapid and significant loss EAT thickness when T2DM patients were treated with liraglutide, a GLP1 analogue, as a result of an increased EAT lipolysis and insulin sensitivity as well decreased lipogenesis (92).

At the level of lipid metabolism, the discovery of an upregulated expression of sterol regulatory element-binding proteins (SREBP) in patients with CAD and diabetic patients, can also represent a new therapeutic target, due its relevance in the control of lipid uptake and lipogenesis (71). Moreover, in 2016, Burgeiro et al. (80) have also shown alterations in EAT lipid metabolism. The results show a decreased lipid metabolism and lipid storage in EAT from patients with heart failure (HF), when compared with SAT biopsies collected from the same HF patients (80).

Insulin-stimulated glucose uptake represents one of the mechanisms responsible for the maintenance of normal blood glucose levels. In AT, it improves the maintenance of normal levels of FFA flux, by promoting lipogenesis, while suppressing lipolysis (93). However, when EAT and SAT samples from HF were compared, the levels of insulin-stimulated glucose uptake were also diminished, independently of diabetic status, a possible indication of insulin resistance development (80) in this subset of patients.

1.5 Mitochondrial Bioenergetics

Mitochondria

Mitochondria are small cytoplasmic organelles that are essential for the maintenance of normal physiological function in cells (94). Each mitochondrium is formed by a double phospholipidic membrane (outer and inner membranes), intermembrane space, cristae and matrix (95). A curious fact about mitochondria is that they carry their own DNA – mitoDNA – that, even though some other proteins are encoded by nuclear DNA, mitoDNA encodes some of the proteins present in the electron transport chain, some of the proteins that are responsible to supply the energy required in cellular processes in the form of adenosine triphosphate (ATP) (95–97).

The electron transport chain is constituted by five enzymatic multi-heteromeric complexes (I – V) that are located in the inner mitochondrial membrane and are responsible for the production of an electrochemical gradient and membrane potential (complex I – IV), that are required for complex V (ATP synthase) activation, that in fact, produces ATP by the conversion of ADP to ATP (98,99).

Complexes I and II receive high energy electrons and protons from hydrogens carriers, as NADH and flavin adenine dinucleotide ($FADH_2$). While the high energy electrons are transferred along the mitochondrial complexes, some energy is lost. Otherwise, this reminiscent energy is used by the complexes to pump protons (hydrogen ions) from the inner side to the intermembrane space, supporting electrochemical gradient maintenance.

In contrast with the first four complexes, complex V is responsible for the re-internalization of hydrogen ions into the matrix, triggering ATP formation by ADP phosphorylation, Figure 9.

To allow the continuous ATP production, it is required not only the permanent donation of high energy electrons but also the removal of the low-energy electrons. Consequently, after the transference along the first four complexes, oxygen acts as the last electron acceptor. This way, an oxygen molecule is reduced, and together with hydrogen ions, water is formed as the final product ($O_2+4e^-+4H^+=2H_2O$).

ATP synthesis as a result of hydrogen carriers oxidation is called oxidative phosphorylation, OXPHOS (98–100). However, accompanied with ATP production, mitochondrial activity allows the formation of several oxidant molecules. Superoxide anion, O^{2-}, represents the first line of ROS, resulting from the reduction of one electron of oxygen. Moreover, O^{2-} is able to react with a wide range of molecules leading to the chemical variety of ROS, as for example nitric oxide (NO) and nitrogen oxygen species (NOS) (101).

Otherwise, side by side with ATP production, some protons can be dissipated from the intermembrane space to the matrix, forcing the mitochondria complex I, II and IV to increase their activity, promoting heat generation (102).

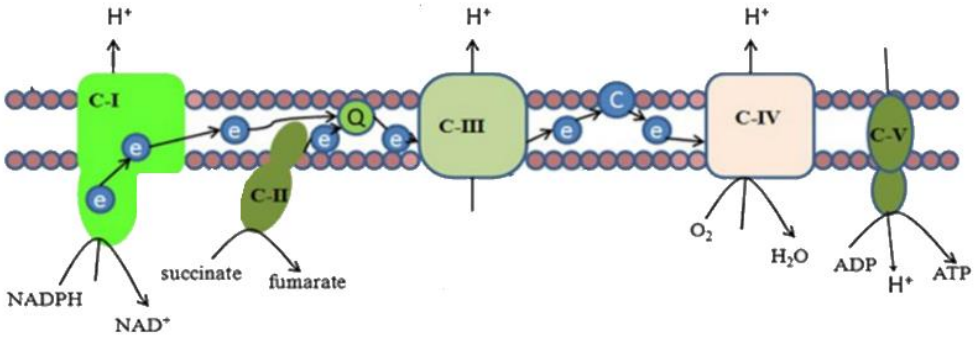

Figure 9. Electron transport chain adapted from (103).

Mitochondria are highly dynamic organelles. Constant alterations in mitochondrial function, number and morphology are required as a response to specific environmental stimuli, which represent their high adaptability to various stimulli (94). Moreover, besides the responsibility to generate ATP, each mitochondrium acts as a key organelle in several metabolic processes. Therefore, the tricarboxylic acid cycle (TCA cycle), glucose homoeostasis and oxidative FA decarboxylation (β-oxidation) are regulated by mitochondria, as well as catabolism of branched amino acids, calcium cycling and regulation of a variety of cell signaling pathways, including cell death (104–108).

Mitochondria and Adipose Tissue

As referred above, mitochondria are present in AT. Furthermore, the increase of mitochondrial proteins represents one of the first steps in adipogenesis (109). This alteration occurs side by side with the lipid droplet accumulation and increased activity of several transcriptional factors related with mitochondrial biogenesis, such as cAMP-responsive element-binding protein (CREB), CCAAT/enhancer-binding protein (C/EBP) family members and PPARγ family (110–113).

The expression of Peroxisome proliferator-activated receptor gamma coactivator 1-alpha (PGC1-α) is essential for adipogenesis. PGC1-α belongs to the PGC1 family of proteins, and it is a coactivator of PPARγ in several genes that are involved in adipogenesis, thermogenesis and mitochondrial biogenesis (114). Thus, the considerable high energy demands required for lipogenesis during adipogenesis are supplied by a strong relation and coordination with mitochondrial biogenesis (114,115).

In mature adipocytes, as well as other cell types, mitochondria support several metabolic processes. A balance between lipogenesis, in the cytoplasm, and FA β-oxidation, in mitochondria, is required to supply all the energy requirements (116).

To produce cytosolic TG, mitochondria contributes with several key intermediates, including glycerol 3-phosphate and acetyl-CoA as result from pyruvate carboxylation and decarboxylation, respectively (117).

After lipolysis, the process that promotes the hydrolysis of TG into glycerol and FFA, the excess of FA released in the cytoplasm is used in mitochondrial β-oxidation, which results not only in energy production, but also as a protective response against lipotoxicity (118–120).

Although, each specific AT shows an individual mitochondrial content that is dependent on its activity. Indeed, when comparing WAT and BAT, there are differences at the mitochondrial level that are followed by particular roles on lipid homeostasis. On BAT, there is an increased expression of uncoupling proteins (UCP). UCP are encoded by nuclear genes and later inserted in the inner mitochondrial membrane (121). Even though, there are five UCP proteins (UCP1-UCP5), UCP1 is the most expressed in BAT, and when activated it functions as an uncoupler, leading to a higher rate of inner membrane proton conductance, that in spite of being used as fuel for ATP production it is dissipated as heat (102). As reviewed by Divakaruni, although there is a basal proton leak in all tissues, that it is independent of UCP as a result of a natural re-entering of H^+ protons into the matrix (122), the heat that is generated by UCP1 activation is much more representative and leads to non-shivering thermogenesis and the maintenance of the core temperature, particularly in neonates (102), figure 10. Curiously, although heat generation, as result of proton leak promote a decrease in ATP production, this process

is completely dependent on lipolysis and consequently β-oxidation followed by OXPHOS (123). Only the activation of the entire pathway allows the electrochemical gradient formation and chemiosmosis required for electron transport activation.

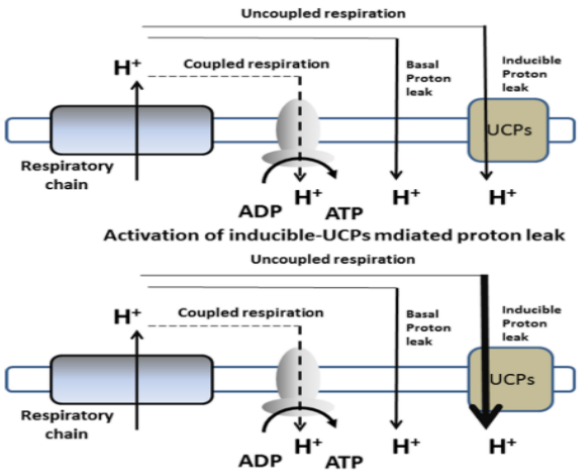

Figure 10. Schematic representation on basal proton leak (on top) and UCP-induced proton leak (on bottom). Adapted from (121).

As mentioned before, beige adipose tissue has functions that may overlap with brown and white adipose cells (42). Although the beige adipocyte origin is not well defined, it is clear that they present a unique transcriptome that leads to both white and brown adipose tissue features, such as large lipid droplets and great thermogenic capacity, respectively (42). Thus, to increase BAT-related genes transcriptions, it is required an environmental alteration is required. A decrease in temperature level or cold environments leads to beige adipocytes activation by white adipocytes "browning" or by pre-beige adipocytes differentiation (124,125). Furthermore, the increased expression of UCP1 leads to heat production in a similar way compared to BAT (39,42,43).

Mitochondria and Epicardial Adipose Tissue

As previously stated, EAT is responsible for a high level of cellular crosstalk that promote heart homeostasis (81). Although considered as a visceral AT, it presents an unique transcriptome with several BAT characteristics, like increased expression of UCP1 and other brown adipocyte factors as PRDM16 and PGC-1α (126).

Thus, mitochondrial populations that are present on EAT can play several roles that are linked with healthy cardiomyocyte function (58). Also, EAT is responsible to supply the high cardiomyocyte with its high energy demands, by influencing the level of circulating lipids and FA release (64,81). Otherwise, BAT-related features are related with control of thermogenesis in the myocardium (65).

Mitochondria are fundamental in Ca^{2+} storage, which is a key feature that it is directly linked with cardiomyocytes. Ca^{2+} currents through cardiomyocyte promote their contractility and consequently blood pumping. However, alterations in EAT mitochondria can influence the Ca^{2+} currents and, as consequence, contractile properties of cardiomyocytes (127,128).

Even though, some studies show how EAT mitochondria can affect cardiomyocyte function (64,65,128), not much is known about the mitochondria capacity in EAT, and how can EAT´s bioenergetics affect cardiomyocyte function.

Mitochondria and Diabetes complications

Mitochondrial alterations can be related with alteration in AT that affecting other tissues. When there are alterations in the ATP supply, FA oxidation, ionic calcium balance and ROS production at the mitochondria level, notorious consequences are observed in the adipocyte and other associated tissues. However, as the various AT depots have different characteristics and the mitochondrial content for each tissue is dependent on its activity and characteristics, dependent on its location.

WAT is closely associated with diabetes and its complications (44); however, BAT may also be involved (129). The thermogenic activity of BAT may be associated with obesity development, in the case of decreased levels of BAT or, even by UCP1 downregulation (130).

The various subtypes of WAT, VAT and SAT, present different lipolytic rates that significantly influence mitochondrial content (106). SAT is considered a tissue with less metabolic activity and represents one of the tissues with more influence in the development of metabolic disorders, such as insulin resistance (131). This occurs mainly because of its high lipid content present in SAT that is only released as FFA when required. Under physiological conditions, SAT can work as a lipid buffer, protecting other

tissues from lipotoxicity (132). Nevertheless, if mitochondria are dysfunctional, the β-oxidation is dysregulated and the amount of FFA in other tissues – the ectopic fat in the muscle and liver, will be increased and several pathways that are related with insulin signaling can be altered (30). Otherwise, VAT is much more active than SAT, presenting higher lipolytic activity. In this tissue, the increased expression of mitochondrial-related proteins is notorious when compared with SAT, including PPARγ (133).

Regarding EAT, mitochondrial dysfunction can also be related with diabetes and metabolic disorders. For example, mitochondria are fundamental in calcium storage; however, a balance between low or high calcium retention is required, since both are related with insulin resistance development. As mentioned above, Ca^{2+} currents are required for cardiomyocyte contractility; in this way, under an insulin resistant state, alterations in the Ca^{2+} currents can affect cardiomyocytes contractile properties, as well as insulin-stimulated glucose transporter 4 (GLUT 4) exocytosis in skeletal muscle cells (127,128).

Adipose tissue mitochondrial metabolism, in particular that of epicardial fat is importantly implicated in cardiac function and in heart physiology. However, not much is known regarding mitochondrial function in adipocytes, and not such studies have date been performed in epicardial adipocytes under diabetes conditions.

Aims

An increasing number of EAT characteristics have been discovered in the last years, mainly anatomic characterization, secretion of bioactive molecules and some studies at the metabolic level.

Very recently evidence shows EAT as a novel therapeutic target for one of the 21st century epidemies, diabetes, and its relationship with the development of diabetic complications, such as CVD, the most lethal of all.

Thus, the overall aim of this study was to characterize EAT, at the level of the insulin signaling pathway, but most importantly to evaluate mitochondrial respiration in epicardial adipocytes and compare it to that of subcutaneous fat, in adipocyte biopsies from subjects with and without diabetes.

For that, the following topics were addressed:

1. Comparison between protein content and protein phosphorylation levels in:
    a. SAT and EAT, under basal conditions
    b. SAT and EAT, under insulin stimuli
    c. SAT and EAT – in the presence or absence of diabetes
2. Comparison between mitochondrial respiration in:
    a) SAT and EAT
    b) SAT and EAT, under UCP1 inhibition and in the presence or absence of diabetes

Chapter 2. Materials and Methods

2.1 Chemicals

Human insulin, Actrapid, 100U/ml Kindly gifted by Novo Nordisk (Paço de Arcos, PT).

The protease inhibitor cocktail (complete Mini) and the phosphatase inhibitor cocktail (PhosSTOP) were obtained from Roche (Carnaxide, PT).

Acrylamid/BisSolution 19:1 (5% c) was obtained from Bio-Rad Laboratories, Inc (Hercules, CA, USA), Bicinchoninic acid (BCA) kit assay and N´, N´, N´, N´ tetramethyllethylenediamine (TMED) from Sigma-Aldrich, Inc (St. Louise, MO, USA), the polyvinylidene difluoride (PVDF) membranes and antibody against total MAPK were purchased from EMD Milipore Corporation (Billerica, MA, USA).

The antibodies against pAKT/PKB (Ser 473), pMAPK (Thr202/Tyr204), p38 (Thr180/Tyr182), FAS and alpha-tubulin were obtained from Cell Signaling Technology, Inc (Danvers, MA, USA), the antibodies against total AKT/PKB and total MAPK were purchased from Upstate EMD Milipore Corporation (Billerica, MA, USA) and the antibody against total p38 MAPK was purchased from Biolegend (San Diego, CA, USA).

Horseradish peroxidase (HRP) secondary antibodies (anti-rabbit and anti-mouse) and the enhanced chemiluminescence (ECL) reagent were purchased from Thermo Fisher Scientific (Waltham, MA, USA).

Methanol, ethanol and isopropanol were obtained from MERCK (Kenilworth, NJ, USA)

All other reagents, including those to prepare Krebs-Ringer HEPES (KHR), relaxing medium (BIOPS) and Mir05 buffers and for high resolution protocols were purchased from Sigma (St. Louis, MO, USA).

2.2 Adipose Tissue donors

This study included 38 subjects with heart failure; 25 were nondiabetic (16 male patients), and 13 had previously been diagnosed with diabetes (8 male patients). Demographic, clinical and biochemical characteristics will be described further in the results, in the Tables 3 and 4. Paired SAT and EAT biopsies were obtained during coronary artery bypass grafting (coronary-artery disease – CAD) or valvular replacement or valvuloplasty (non-coronary artery disease – NCAD) surgery. EAT was collected from the proximal right artery and SAT from the sternum region (80). The study was performed after the following inclusion criteria: a) To be 18 years or older; b) Written

consent from participants and c) Protocol approved by the Ethical Committee of the University Hospital of Coimbra. Studies were carried out in accordance with the Declaration of Helsinki. The exclusion criteria: a) Renal failure (serum creatinine ≥2 mg/dL or need for hemodialysis); other metabolic diseases; or other diseases known to significantly decrease life expectancy and/or to alter the inflammatory cascade activation, such as cancer or Parkinson, for example.

2.3 Specific Adipose Tissue storage

After collection of human adipose tissue samples, each assay demands a specific methodology for tissue storage or maintenance. For mRNA, EAT and SAT were stored in a 2ml tube containing 1ml of RNALater® and immediately frozen in dry ice. For evaluation of protein expression, AT biopsies were kept in 6mM glucose KHR at 37º. KHR buffer was prepared with 4% bovine serum albumin (BSA), 140 mM sodium chloride (NaCl), 4.7mM potassium chloride (KCl), 1.25 mM magnesium sulfate ($MgSO_4$), 126 mM calcium chloride ($CaCl_2$), 5.8 mM sodium phosphate NaH_2PO_4), 200 nM adenosine deaminase, and 25 mM HEPES, pH 7.4, adjusted with NaOH. For high resolution respirometry (HRR), using the Oroboros technology, paired EAT and SAT samples were kept in relaxing medium (BIOPS) at 4°C. BIOPS buffer was prepared with, 10 mM containing Ca^{2+}/EGTA buffer (free calcium 0.1 μM), 20 mM imidazole, 50 mM K^+/4-morpholinoethanesulfonic acid, 0.5 mM dithiothreitol, 6.56 mM $MgCl_2$, 5.77 mM ATP,15 mM phosphocreatine, pH 7.1, adjusted with HCl.

2.4 Adipose tissue protein expression

2.4.1 Insulin stimulation and lysates preparation

After 2 washes in KHR buffer, adipose tissue was cut into small pieces (around 0.5 mm) and transferred to KHR without glucose and stimulated or not with human insulin (1000 μU/ml) for 10 min in a shaking water bath (60 bpm), as previously reported (80). Following insulin stimulation, SAT and EAT biopsies were homogenized in ice-cold RIPA buffer 20 mM Tris HCL (pH 7,4), 25mM NaCl, 1% NP-40 (Nonidet p-40), 5 mM EADTA, 10mM Sodium diphosphate ($Na_4P_2O_7$), 10 mM Sodium fluoride (NaF), 2 mM Sodium Vanadate, 10μg/ml Aprotinin from bovine lung, 1mM Benzadamidine and 1 mM phenylmethylsulfonyl (PMSF) (1:1 dilution) and homogenized three times, during 5 sec, at 13500 rpm using ULTRA-TURRAX T 25 basic, IKA®-Weke (Staufen, Germany)

homogenizer, to disrupt cells. Samples were then centrifuged twice at 12000 rpm at 4°C for 10 min and the supernatants were collected.

2.4.2 Protein concentration determination by the BCA method

The BCA method, also known as "biuret method" is a copper-based protein assay used for protein quantification, whereby peptides containing three or more amino acid residues form a colored chelate complex with Cu^{2+}, in an alkaline environment containing sodium potassium tartare. The recognized purple color results from chelation of two molecules of BCA with one cupreous ion and this solution can be read by a spectrophotometer, at 540-570nm, in a time-depend manner. Although, to determine protein content, sample absorption needed to be compared with protein standards and a standard curve is needed. Indeed, at the time, the absorption of bovine serum albumin (BSA) of increasing concentration between 12.5μg mL^{-1} and 800μg mL^{-1} was determined and used as a standard linear curve to determine protein concentration, at the same time. Equal amounts of diluted proteins samples (1:10) and water or BSA dilution and the sample buffer RIPA in a final volume of 50μL were placed in a 96 multi-well plate. Then 200μL of BCA reagent was added to the wells and the plate was incubated in the dark for 30 min, at 37°C. After incubation, the absorption was measured in an automatic microplate reader (SLT, Austria) at 570nm. This method is not affected by a range of detergents and denaturing agents such as urea and guadinidinium chloride, although it is more sensitive to the presence of reducing sugars (134).

2.4.3 Immunoblotting

Western Blot (WB) analyses was used to determine cellular protein levels, providing information about proteins expression, in addition to their phosphorylation levels through the use of specific antibodies against these phosphorylated forms, indicating activation of the signaling pathways involved.

Thirty micrograms of proteins lysates from each sample were mixed with sample buffer (0.125mM Tris pH 6,8; 2% w/v SDS; 100 mM DTT; 10% Glycerol and bromophenol blue), denatured at 90°C and loaded onto a 7,5 or 10% (V/V) sodium dodecyl sulfate polyacrylamide gel electrophoresis (SDS-PAGE), according to the specific molecular weights. Then, separated proteins were transferred to a polyvinylidene fluoride (PVDF) membrane. To confirm equal amount of protein in each well and "bubble" absence, the

PVDF membrane is submersed in Ponceau solution for staining and then blocked with Tris buffer with 0.02% of Tween 20® (TBS-T, pH 7,4) containing 5% BSA for 1h at room temperature. Later, membranes were incubated overnight at 4°C with the primary antibodies shown on Table 1, as well as, respective dilution, according to manufacturer instructions.

Table 1. List of antibodies used for Western blot and respective dilutions.

Antibody	Dilution
P -AKT/ PKB (Ser 473)	1:1000
Total AKT/PKB	1:1000
P- p38 MAPK (Thr180/Tyr182)	1:000
Total p38 MAPK	1:1000
P-MAPK (Thr202/Tyr204)	1:1000
Total MAPK	1:1000
Total FAS	1:1000
Alpha-tubulin	1:5000

The following day, membranes were washed three times for 15min with TBS-T and incubated during 1h at room temperature with the specific secondary antibody.

Secondary antibodies (Thermo Fisher Scientific) were linked to horseradish peroxidase (HRP) and complexes were detected after exposure to ECL, for 2 min followed by scanning on ChemiDoc™ Imaging System, Bio-Rad (Bio-Rad Laboratories, Amadora, Portugal).

The generated signals were quantified using the FIJI® Software and relative protein expression was normalized to the α-tubulin antibody. The normalization protein used was selected based on our previous results demonstrating that it does not change

under these conditions. Subsequently, the values were normalized to control (no-treated SAT, NDM) for each membrane.

2.5 Mitochondrial respiration

2.5.1 Oxygraph-2k respirometer calibration

All oxygen consumption measurements were performed as recommended by Oroboros Instruments (Innsbruck, Austria) (135,136) using a high resolution Oxygraph-2k respirometer, Figure 11.

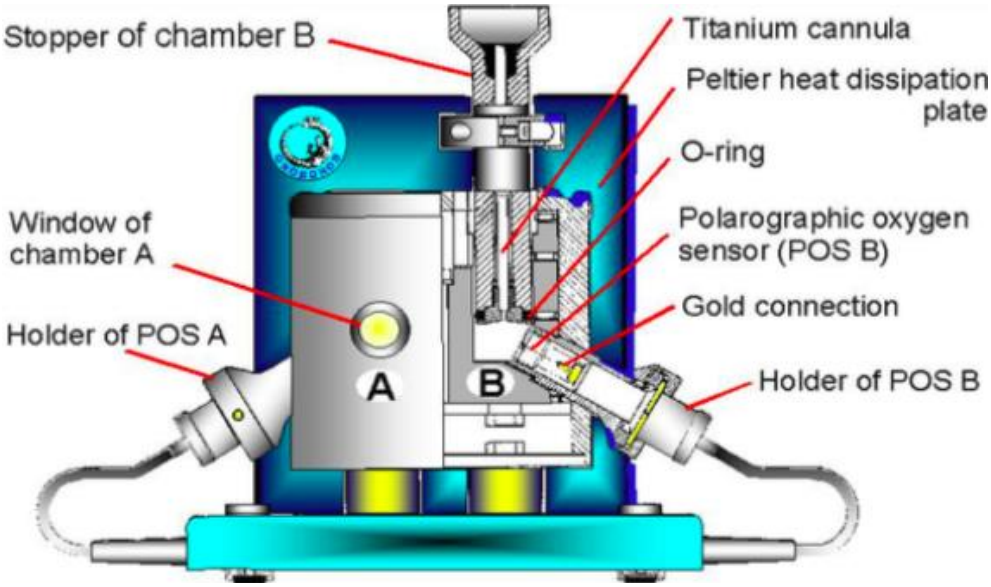

Figure 11. The Oroboros Oxygraph (135).

Before each experiment, a background calibration was performed for each chamber where a O2K polygraphic oxygen sensor (POS) is installed (Figure 11). This calibration was performed in MirO5 buffer solution (110 mM sucrose, 60 mM potassium lactobionate, 0.5 mM EGTA, 3 mM $MgCl_2.6H_2O$, 20 mM taurine, 10 mM KH_2PO_4, 20 mM Hepes, 1 g/L BSA pH 7.1 at 37°C) at atmospheric oxygen concentration. The temperature was maintained at 37°C by an electronic Peltier during background calibration, as well as during all HRR experiments.

2.5.2 Sample preparation

After biopsy collection, tissue samples were immediately immersed in ice-cold relaxing medium (BIOPS). Samples were transported to the laboratory on wet-ice within an hour.

In the laboratory, the biopsies were slightly dried and weighed, approximately 50 mg of SAT and EAT explants (cut into small pieces) were entered into the cambers in 2.0 mL of Mir05 and were monitored in the Oxygraph-2k respirometer under controlled temperature (37°C) and stirring (750 rpm). Part of the biopsy was frozen in liquid nitrogen and stored at –80°C for later analysis of mitochondrial DNA.

2.5.3 Respirometry protocol

To evaluate mitochondrial capacity, substrate-uncoupler-inhibitor titration (SUIT) protocols were used. SUIT protocols represent a variety of experimental conditions designed to evaluate mitochondrial function in coupling control sates of LEAK, OXPHOS and electron transfer (ET) capacity (136).

There are a wide range of SUIT protocols, regarding the tissue, as well as the sample type: isolated mitochondria, permeabilized or intact cells and tissue homogenates (136). Reference protocol 2 (RP2) (Table 2) was used to measure EAT and SAT mitochondrial respiration, in regard to the mitochondrial electron transfer capacity and OXPHOS; however, no Leak is measured under these conditions (136).

All assays were started with an initial oxygen concentration of 400 nmol ml^{-1}. Oxygen consumption reflects the first derivative of the oxygen concentration (nmol/ml) in time in the respiration chambers and is termed oxygen flux [pmol/(s*mg)], corrected for the wet weight of the adipose tissue (≈ 50 mg) introduced into the chamber. For evaluation of the OXPHOS parameters, substrates/uncoupler/inhibitors were injected into the recording chamber as described in Table 2. Digitonin was added to the chamber in the beginning to permeabilize cells and baseline respiration or residual oxygen consumption (ROX) was recorded before subsequent addition of substrates and measurements of oxygen consumption. The concentration of digitonin (2 µM) was chosen taking into account previous studies (101,137). After cell membrane permeabilization, GDP was added to inhibit UCP1 (138), mainly in the EAT tissue (40). Then, the early addiction of ADP and Malate.1 (Mal.1) promoting the saturation of endogenous substrates by kinetically saturation of OXPHOS activity without overestimation of the OXPHOS-pathway activity. Octanoylcarnitine (Oct) was then added, promoting the stimulation of fatty acid (FA) oxidation and consequently OXPHOS activity stimulated by NADH-pathway and the F pathway.

After testing cell membrane integrity using Cytochrome c (Cyt c), the reconstitution of the TCA cycle by titration of Pyruvate (prepared fresh daily), Malate and Glutamate, promoting the induction of the OXPHOS pathway mediated by Complex I activity. To evaluate the effect of complex II to OXPHOS, a saturating concentration of Succinate was added to the chambers, combining OXPHOS mediated by FA oxidation, Complex I and Complex II substrates.

The maximal coupled oxidative capacity with convergent electron input through complex I and II was obtained after adding succinate. Then, carbonyl cyanide m-chlorophenyl hydrazone (CCCP) was titrated to obtain maximal uncoupled respiration of the respiratory chain activity. Then to obtain complex inhibition, specific inhibitors were added. Rotenone (Rot) was added to inhibit complex I, thus only complex II activity was then measured, followed by Antimycin A (AA) for complex III inhibition, and thus a measurement of chemical residual oxygen consumption was possible. Finally, to evaluate the activity of complex IV in the Electron Transfer coupling state, titration of Ascorbate (Asc) + TMPD was performed.

Table 2. A list of substrates, uncoupler and inhibitors used for high respiration, as well as their respective concentration and respiratory states.

Substrate/Inhibitor	Stock Concentration	Final Concentration	Pathway control and Respiratory states
Digitonin	8,1mM	8,1µM	ROX
GDP	0,2M	1mM	
ADP	0.5M	7,5µM	
Mal.1	50mM	0,1M	
Oct	100mM	0,5µM	F(Oct)p
Cyt c	4mM	10µM	F(Oct)pc
Pyruvate	2M	5mM	FN(OctPMG)p
Malate	0,8M	1,9mM	
Glutamate	2M	5mM	
Succinate	1M	50mM	FNS(OctPMG)p
CCCP	1mM	0,5 µM; 0,25µM	FNS(PMG)e
Rot	2,5M	2,5µM	Se
AA	5mM	12,5µM	ROX
Asc	0,8M	2µM	CIV
TMPD	200mM	0,5µM	

GDP: Guanosine diphosphate; ADP: Adenosine diphosphate, Oct: octanoylcarnitine, PMG: pyruvate, malate and glutamate; Succ: succinate; CCCP: Carbonyl cyanide 3-chlorophenyl hydrazone; Rot: rotenone, AA: antimycin A; Asc+TMPD: ascorbate and tetramehyl-p-phenylenediamine. ROX: residual oxygen consumption, F(Oct)p: addiction of octanoylcarnitine for stimulation of fatty acid – OXPHOS (F-OXPHOS) pathway; F(Oct)pc: Cyt c test for cell integrity membrane ;FN(OctPMG)p: stimulation of NADPH-pathway and F-OXPHOS, by second addiction of malate and pyruvate and glutamate; FN- OXPHOS; FNS(OctPMG)p: Succ addiction for stimulation of FN- OXPHOS by complex II; FNS(PMG)e: Electron transfer (ET) coupling state, evaluated after CCCP titration for noncoupled state of maximum respiration on FNS-OXPHOS; Se: Evaluation of ET coupling state after complex I inhibition by Rot ; ROX: AA addiction for chemical evaluation of residual oxygen consumption; CIV: Asc+TMPD to evaluate CIV activity in the ET coupling state.

2.6 Statistical Analysis

For normally distributed data, a parametric t-test was performed, whereas for non-normally distributed data the Mann-Whitney nonparametric test was used. In the case of categorical variable, we used the chi-squared tests. Statistical tests were performed using the SPSS software (version 24), with a significance level of 0, 05. To verify if the data followed a normal distribution we used the Kolmogorov-Smirnov test. Since the data did not follow a normal distribution we resorted to the Mann-Whitney U non-parametric test. To assess the role of tissue type or disease status on quantitative variables, nonparametric multivariate ANOVA tests was performed. The level of significance consider throughout the analysis was 0,05, i.e., the differences were considered significant if $p < 0,05$.

Data comparing EAT *versus* SAT from NDM patients, due to the small number of samples (n) involved, no statistical analysis was performed; EAT *versus* SAT and NDM *versus* DM protein expression, are presented with means and SD, when possible; mitochondrial respiration data EAT *versus* SAT and NDM *versus* DM are presented as median and moderate outliers, shown as circles in box-and-whisker plots in figures related with mitochondrial respiration and insulin signaling proteins analysis, lie more than one and a half times the interquartile range (IQR), that is, below Q_1 - 1.5 X IQR or above Q_3 + 1.5 X IQR.

Chapter 3. Results

EAT is a specific type of VAT that surrounds almost 80% of the heart surface (54,55). Under physiologic conditions, it is responsible for the secretion of a variety of bioactive molecules that can regulate metabolic and immune functions, with protective effect to cardiomyocytes and coronary arteries (68,69). Like other fat depots, EAT has high plasticity and its thickness undergoes constant volume adaptation and, consequently, alteration in adipocyte number and size, in response to aging, diet, drugs and pathologies, such as DM (87). Under obesity conditions or T2DM, EAT undergoes expansion with a consequent abolishment of EAT´s protective effects to the heart. As other fat tissues, the increase in adipocyte size and number can lead to the upregulation of several adipokines that can promote pro-inflammatory and injury to the myocardium (68,79,80). These metabolic alterations may affect several metabolic pathways, such as FA oxidation and cardiac metabolism by the modulation of FA uptake, insulin signaling and insulin-mediated glucose uptake (74,80,139). The increased cardiac pool on lipotoxic species and ROS may lead to mitochondrial dysfunction, causing, in turn, cardiomyocyte contractile dysfunction, promoting heart failure (84). Despite the important physiological role of EAT in cardiovascular metabolism, few studies have been carried out in order to evaluate its therapeutic potential.

3.1Characterization of Adipose Tissue donor

From the 38 patients with heart failure (HF) enrolled in this study, 25 were non-diabetic (NDM) and 13 were diabetic (DM) patients. Of the 25 NDM subjects most presented level II in the New York Heart Association (NYHA) functional classification of HF, level II in the Canadian Cardiovascular Society (CCS) functional classification of angina, left ventricle ejection fraction (LVEF) ≥ 50%, and left shortening fraction (LVSF) ≥ 27% (Table 3). Among the DM patients, most presented level II-III in the NYHA functional classification and equal distribution of CSS functional classification of angina, LVEF ≥ 50%, and LVSF ≥ 27% (Table 3).

Compared with DM patients, NDM subjects show higher percentage of cardiovascular risk factors, such as hypertension and dyslipidaemia (Table 3). Although, diabetic patients were, in generally, under hyperglycaemic control and medication, fasting blood glucose was significantly increased in diabetic patients compared to NDM

subjects (100,72 ± 2,28 vs 156,62 ± 11,45; p<0,001, Table 4). In addition, Table 3 also describes the various medications taken by the study cohort.

Table 3. Demographic and clinical and characteristics of the study population.

	Non-diabetic patients	Diabetic patients	*p* value
N	25 (65,79%)	13 (34,21%)	
Male (%)	64%	61,5%	0,850
BMI, Kg/m² (mean ± SEM)	26,91 ± 0,70	27,73 ± 0,82	0,597
Risk factors (%)			
Hypertension	84	69,23	0,190
Dyslipidemia	84	69,23	0,190
Blood pressure, mm/Hg (mean ± SEM)			
Systolic	128,2 ± 3,32	133,09 ± 6,23	0,292
Diastolic	69,48 ± 2,52	66,45 ± 3,15	0,342
Medications (%)			
Antiplatelet	32,00	23,07	0,490
Anticoagulant	20,00	38,46	0,060
Antidiabetic			
Insulin	-----	38,46	
Metformin	-----	46,15	
DPP4 inhibitor	-----	7,69	
DPP4 inhibitor + Biguanide	-----	30,76	
ACEI	36,00	76,92	0,003
β blocker	60,00	76,92	0,125
Calcium channel blocker	12,00	15,38	0,759
Diuretic	68,00	30,76	< 0,001
Statins	72,00	76,92	0,811
NHYA Functional Classification of Heart Failure (%)			
I; I-II	4;4	0;0	
II; II-III	20;12	7,69; 53,85	
III; III-IV	12;12	7,69;0	
IV	0;4	0;0	
CCS Functional Classification of Angina (%)			
I; I-II	0;0	0;0	
II; II-III	24;4	7,69;7,69	
III; III-IV	4;0	7,69;0	
IV	0,00	0,00	
LVEF (%) (≥ 50%)	55,55	86,96	0,001
LVSF (%) (≥ 27%)	100,00	100,00	0,990

Quantitative measurements are presented as means ± SEM, and qualitative parameters are presented as percentage, BMI, body mass index; ACEI, angiotensin-converting enzyme inhibitor; NYHA, New York Heart Association; CCS, Canadian Cardiovascular Society; DPP-4 dipeptidyl peptidase-4; LVEF, left ventricle ejection fraction; LVSF, left ventricle shortening fraction. For normally distributed data, a parametric t-test was performed, whereas nonparametric Mann-

Whitney test was applied for nonnormally distributed data. $p < 0,05$ was considered significant. For categorical variables, a X^2 was applied.

Table 4. Biochemical characteristics of the study population

Metabolic biochemical parameters	Non-diabetic patients	Diabetic patients	*p* value
Fasting glucose (mg/dl)	100,72 ± 2,28	156,62 ± 11,45	<0,001
Kidney biochemical parameters (mg/dl)			
Urea	25,52 ± 3,91	25,5 ± 5,91	0,902
Creatinine	1,19 ± 0,30	1,04±0,09	0,456
Liver biochemical parameters (U/l)			
GOT	25,09 ± 1,89	51,38 ± 21,19	0,836
GPT	24,68 ± 3,30	53,22 ± 25,93	0,535
GGT	40,14 ± 5,65	83,13 ± 52	0,615
ALP	76,86 ± 5,17	75,86 ± 10,19	0,793
LDH	255,63 ± 18,19	262,4 ± 47,39	0,945
CK (U/l)	91,43 ± 9,69	250 ± 118,13	0,24

Data are presented as means ± SE. GPT, glutamic pyruvic transaminase; GOT, γ-glutamyl transferase; ALP, alkaline phosphatase; LDH, lactate dehydrogenase; CK, creatine kinase. For normal distributed data, a parametric t-test was performed, whereas a nonparametric Mann-Whitney U test was applied for non-normally distributed data. $p<0,05$ was considered significant.

3.2 Expression of insulin signaling related proteins in EAT and SAT from HF patients

Previous studies carried out in our lab showed that EAT adipocytes have lower glucose uptake under insulin stimulation per cell, per second, when compared with SAT adipocytes, however this tissue has smaller but many more cells than SAT does per mg of tissue (80,140). To date, there are no studies evaluating insulin signaling in these cells and how this could influence EAT homeostasis and metabolism.

Therefore, EAT and SAT explants from NDM and DM patients were subjected to insulin treatment for 10 minutes and AKT/PKB phosphorylation levels on Ser 473 and total AKT/PKB protein expression levels were evaluated (Figure 12). AKT/ PKB is a key protein kinase that is involved in insulin metabolism in insulin-sensitive tissues (adipose tissue, liver and muscle), and it is responsible for the regulation of hepatic glucose production (141). Indeed, AKT/PKB deficiency can lead to lipodystrophy (142) or insulin resistance and DM development in mice (143). Moreover, insulin stimulation of AKT/PKB phosphorylation on Ser 473 was impaired in brown adipocytes after treatment with rapamycin, an immunosuppressive agent that contributes to new onset diabetes after transplantation (NODAT) (144).

So far, the results obtained from NDM patients (Figure 12 A - G), in either tissue, show increased AKT/PKB phosphorylation on Ser 473 after insulin stimulation, in SAT 120,80% and in EAT 86,94%. When comparing the two tissues, AKT/PKB phosphorylation is increased in EAT, either in the basal by 88,4% and by 59,5% after insulin stimulation, Table 5. In addition, total AKT/PKB protein expression was also evaluated in SAT *versus* EAT and it was increased in EAT by 46,81%, Table 5.

Table 5. Relative differences on AKT/PKB phosphorylation on Ser 473 and total AKT/PKB expression from NDM patients.

	SAT			EAT			SAT Vs EAT	
	B (Mean±SD)	I (Mean±SD)	B Vs I (%)	B (Mean±SD)	I (Mean±SD)	B Vs I (%)	B (%)	I (%)
P- AKT/PKB (n=3)	1,000±0,290	2,208±0,361	120,8%	1,884±0,285	3,552±0,261	86,94%	88,4%	59,51%
Total AKT/PKB (n=3)	1,002±0,074			1,471±0,411			46,81%	

B: basal; I: insulin stimulated. Relative differences in AKT/PKB phosphorylation on Ser 473 in SAT and EAT from NDM patients were calculated considering the basal from each tissue as 100%; Relative differences in the insulin effect in SAT versus EAT from NDM patients was calculated considering SAT with insulin stimulation as 100%; Relative differences on total AKT/PKB expression was calculated, considering SAT as 100%.

On Figure 12 K, when AKT/PKB phosphorylation on Ser 473 in NDM *versus* DM patients was analyzed, in NDM patients, AKT/PKB phosphorylation on Ser 473 was increased by 106,7% in SAT and in EAT the increase is subtler 26,29%, Table 6.

The results obtained from AKT/PKB phosphorylation on Ser 473 in SAT and EAT from DM patients indicated increased phosphorylation of AKT/PKB after insulin stimulation by 85,29% in SAT, and a slight increase of AKT/PKB phosphorylation by 27,98% in EAT, as shown in Table 6. When the values from EAT and SAT after insulin stimulation were compared, SAT shows 27,98% higher AKT/PKB phosphorylation than EAT, Table 6. No differences on total AKT/PKB were found when SAT and EAT from NDM and DM patients, Table 6.

When our preliminary results of AKT/PKB phosphorylation on Ser 473, from SAT and EAT (from either NDM and DM) were compared, Table 6, DM patients show a slight decrease either in the basal state, by 18,40% in SAT and by 28,54% in EAT, as well as after insulin stimulation by 15,71%, however, when SAT values (either from NDM and DM patients) were compared in the presence of insulin, NDM show a slight increase by 26,85% in AKT/PKB phosphorylation compared to DM.

Quantification of phosphorylated and total AKP/PKB, as well as Phospho-AKT/Total AKT ratio are shown on Figure 12 H-J.

Table 6. Relative differences on AKT/PKB phosphorylation on Ser 473 and total AKT/PKB expression from NDM and and DM patients.

	NDM SAT (n=3)			NDM SAT Vs DM SAT (%)		NDM EAT (n=3)			NDM SAT Vs EAT		NDM EAT Vs DM EAT (%)	
	B (Mean±SD)	I (Mean±SD)	B Vs I (%)	B (%)	I (%)	B (Mean±SD)	I (Mean±SD)	B Vs I (%)	B (%)	I (%)	B (%)	I (%)
P - AKT/ PKB (n=3)	1,000 ± 0,000	2,067± 1,340	106,7%			1,023± 0,350	1,292± 0,291	26,29 %	2,30%	37,49 %		
Total AKT (n=2)	0,900±0,241					0,8249±0,360			8,35%			
	DM SAT					DM EAT			DM SAT Vs EAT			
	B (Mean±SD)	I (Mean±SD)	B Vs I (%)	B (%)	I (%)	B (Mean±SD)	I (Mean±SD)	B Vs I (%)	B (%)	I (%)	B (%)	I (%)
p- AKT/ PKB (n=3)	0,816± 0,565	1,512± 1,074	85,29%	18,40 %	26,85 %	0,731± 0,325	1,089± 0,386	48,75 %	10,42 %	27,98 %	28,54 %	15,71 %
Total AKT (n=2)	0,802±0,524			10,93%		0,700±0,407			O,86%		3,62%	

B: basal; I: insulin stimulated. Relative differences in AKT/PKB phosphorylation on Ser 473 in SAT and EAT from either NDM and DM patients were calculated considering the basal from each tissue as 100%, respectively from NDM and DM patients; Relative differences in SAT versus EAT from NDM patients was calculated considering SAT from NDM, patients with insulin stimulation, as 100%, in DM patients SAT from DM, with insulin stimulation was considered as 100%; Relative differences on total AKT/PKB expression was calculated, considering SAT as 100%.

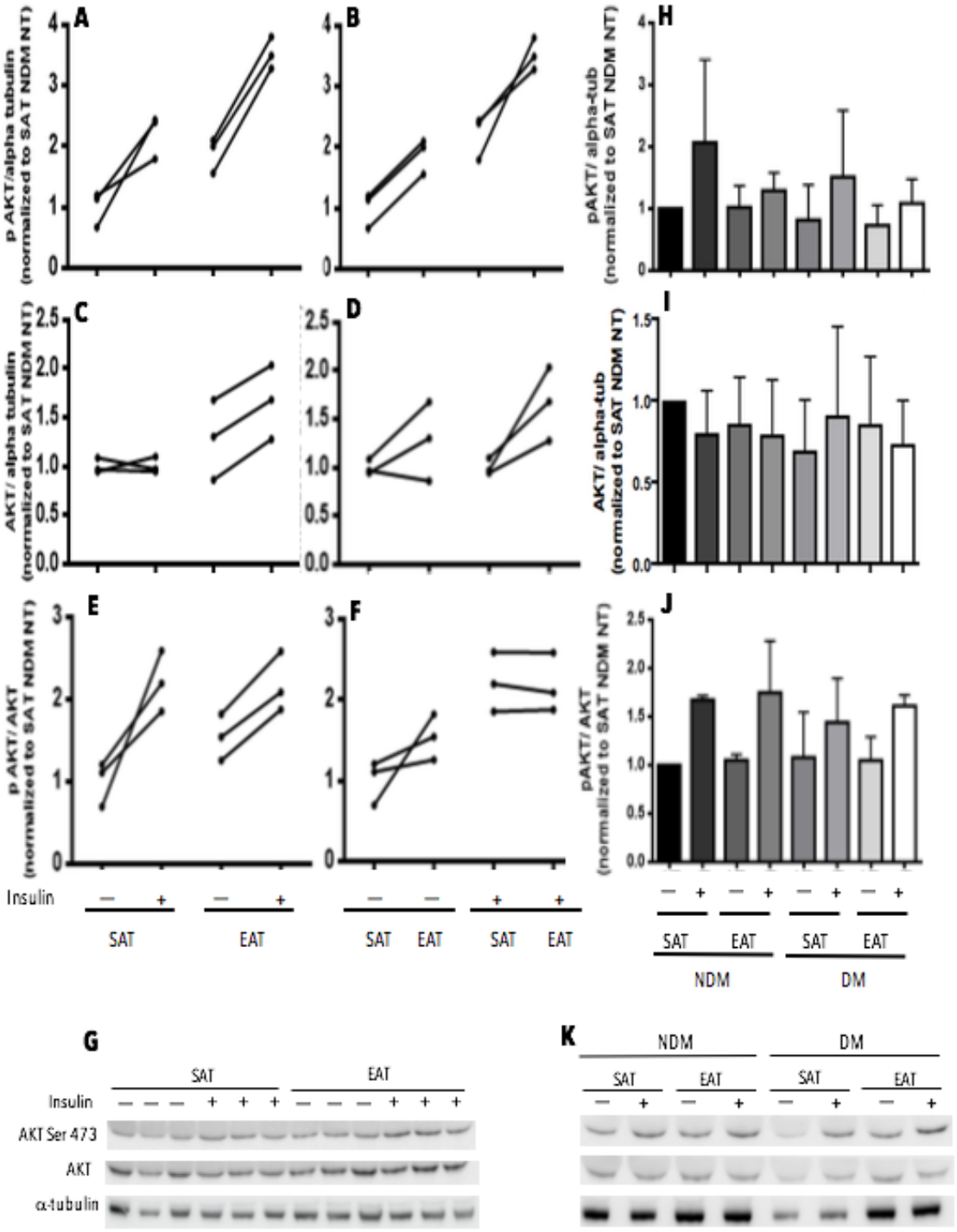

Figure 12. AKT/ PKB content and phosphorylation levels in EAT and SAT from HF patients, with and without DM. 30μg of protein obtained from tissue explants from NDM patients **(G**) and NDM *versus* DM patients **(K)** was subjected to SDS-PAGE, transferred to a PDVF membrane and then to WB. EAT and SAT specific relative differences, with and without insulin stimulation, on phosphorylation level of AKT/PKB (Ser 473) (n=3) and total AKT/PKB expression level (n=3) in NDM **(G)** and in NDM versus DM patient phosphorylation level of AKT/PKB (Ser 473) (n=3) and total AKT/PKB expression level (n=2). **(K)** were analysed. Signal quantification from total and phosphorylated AKT/PKB (Ser 473) on NDM **(A, B, C, D, E, F)** and NDM *versus* DM **(H, I, J)** was obtained using FIJI program, and values were corrected by normalization with α-tubulin and to the control (SAT from NDM patients without insulin stimulation). Results were presented as mean ± SD on line graphs.

Although a small number of patients, our preliminary results demonstrate that insulin stimulation increased in AKT/PKB phosphorylation in both tissues; however, more experiments are needed in order to increase the "n" for each condition. Insulin was able to phosphorylate AKT/PKB in both tissues, this activation was measured per microgram of protein loaded and not per cell as was the case in the experiments that measured the insulin-stimulated glucose uptake in these tissues.

In adipocytes, mitogen activated protein kinases (MAPK) (ERK 1/2), p38 and c-Jun N-terminal kinases (JNK) are different MAPK that are involved in adipocyte differentiation and maturation (145). However, these three MAPK families are involved in different cellular functions: on the one hand, MAPK (ERK 1/2) are usually activated by mitogens or growth factors, including insulin, and its activation can lead to cell proliferation; on the other hand, p38 and JNK are activated under several stress stimuli, and their activation can induce apoptotic responses (145–147). Nevertheless, no studies have measured the expression of these MAPK proteins in EAT adipocytes. In order to evaluate MAPK protein levels in EAT and SAT adipocytes, fat cell explants from both tissues were analyzed, Figure 13. Our preliminary results indicate that there are no evident preliminary differences in total MAPK protein levels or in MAPK phosphorylation levels on Thr 202/Tyr 204 residues in the two fat tissues studied (Figure 13 A - G).

In Figure 13 G, there was no difference in MAPK phosphorylation when comparing before and after insulin stimulation in either tissue, although in both tissues there was a slight decreased after insulin stimulation: by 22,65% in SAT and by 12,20% in EAT. When SAT and EAT were compared under basal condition and after insulin treatment, EAT shows a decreased by 40,20% in basal state and by 32,02% after insulin stimulation in EAT, Table 7. Total MAPK protein levels are 16,69% more expressed in SAT than in EAT.

Table 7. Relative differences on MAPK phosphorylation on Thr202/Tyr204 and total MAPK expression from NDM patients.

	SAT			EAT			SAT Vs EAT	
	B (Mean±SD)	I (Mean±SD)	B Vs I (%)	B (Mean±SD)	I (Mean±SD)	B Vs I (%)	B (%)	I (%)
P- MAPK (n=3)	1,000±0,321	0,774±0,072	22,65%	0,598±0,110	0,525±0,023	12,20%	40,2%	32,09%
Total MAPK (n=3)	1,000±0,258			0,8331±0,096			16,69%	

B: basal; I: insulin stimulated. Relative differences in MAPK phosphorylation on Thr202/Tyr204 in SAT and EAT from NDM patients were calculated considering the basal from each tissue as 100%; Relative differences in the insulin effect in SAT versus EAT from NDM patients was calculated considering SAT with insulin stimulation as 100%; Relative differences on total MAPK expression was calculated, considering SAT as 100%.

On the other hand, our preliminary results, in Figure 13 K, indicate more protein phosphorylation and expression in EAT than in SAT, in either NDM and DM, further experiments need to be done in order to obtain a robust and final conclusion. However, after normalization of the results with α-tubulin, the preliminary results show no differences in MAPK phosphorylation from NDM and DM in EAT, either in basal state, by 1,14% increase in DM, as well as after insulin stimulation by 10,61% compared to DM patients; although in the basal state, SAT show a decrease by 12,48% in DM patients, after insulin stimulation there are an increase by 47,31% in SAT from DM compared to NDM, when compared to NDM. When total MAPK protein expression in SAT and EAT, either from NDM, and DM patients, after the normalization referred above, no differences were observed in SAT (0,55%), although in EAT, total MAPK expression is a slight decreased in DM patients, 21,34%, Table 8.

Quantification of phosphorylated and total MAPK, as well as Phospho-MAPK/Total MAPK ratio are shown on Figure 13 A-J.

Table 8. Relative differences on MAPK phosphorylation on Thr202/Tyr204 and total MAPK expression from NDM and

DM patients.

	NDM SAT			**NDM SAT Vs DM SAT (%)**		**NDM EAT**			**NDM SAT Vs EAT**		**NDM EAT Vs DM EAT (%)**	
	B (Mean±SD)	I (Mean±SD)	B Vs I (%)	B (%)	I (%)	B (Mean±SD)	I (Mean±SD)	B Vs I (%)	B (%)	I (%)	B (%)	I (%)
P-MAPK (n=1)	1,000	0,463	53,67%			0,863	0,920	6,52 %	13,70 %	37,49 %		
Total MAPK (n=2)	0,900±0,241					0,682±0,160			23,78%			
	DM SAT					**DM EAT**			**DM SAT Vs EAT**			
	B (Mean±SD)	I (Mean±SD)	B Vs I (%)	B (%)	I (%)	B (Mean±SD)	I (Mean±SD)	B Vs I (%)	B (%)	I (%)	B (%)	I (%)
P-MAPK (n=1)	0,876	0,682	22,07%	12,40 %	47,31 %	0,886	0,822	7,18 %	1,14%	27,98 %	2,66 %	10,61 %
Total MAPK (n=2)	0,890±0,099			O,55%		0,536±0,051			39,72%		21,34%	

B: basal; I: insulin stimulated. Relative differences in MAPK phosphorylation on Thr202/Tyr204 in SAT and EAT from either NDM and DM patients were calculated considering the basal from each tissue as 100%, respectively from NDM and DM patients; Relative differences in SAT versus EAT from NDM patients was calculated considering SAT from NDM, patients with insulin stimulation, as 100%, in DM patients SAT from DM, with insulin stimulation was considered as 100%; Relative differences on total MAPK expression was calculated, considering SAT as 100%.

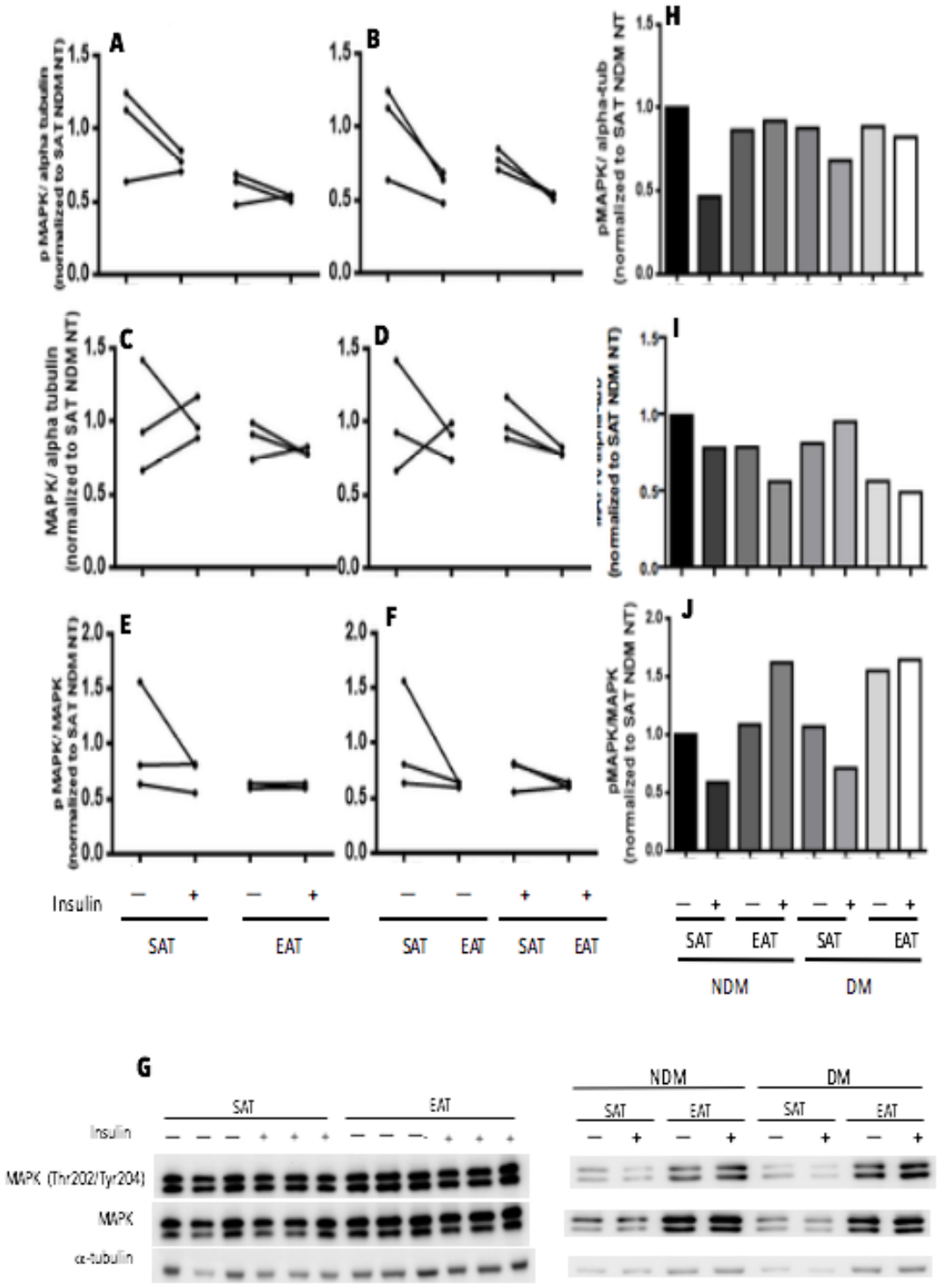

Figure 13. MAPK content and phosphorylated levels in EAT and SAT from HF patients, with and without DM. 30µg of protein obtained from tissue explants from NDM patients **(G**) and NDM *versus* DM patients **(K)** was subjected to SDS-PAGE, transferred to a PDVF membrane and then to WB. EAT and SAT specific relative differences, with and without insulin stimulation, on phosphorylation level of MAPK (Thr 202/Tyr 204) (n=3) and total MAPK protein level (n=6) **(G)** and in NDM versus DM patient on phosphorylation level of MAPK (Thr 202/Tyr 204) (n=1) and MAPK protein level (n=1) **(K)** were evaluated. Relative protein expression was corrected by normalization with α-tubulin. Signal quantification from total MAPK and its phosphorylated form on Thr 202/Tyr 204 in NDM **(A, B, C, D, E, F)** and in NDM *versus* DM **(H, I, J)** was obtained using FIJI program, and values were corrected by normalization with α-tubulin and to the control (SAT from NDM patients without insulin stimulation). Results were presented as mean on line graphs.

As referred to above, not all MAPK proteins mediate cell proliferation. In fact, p38 is a protein that is activated in the presence of several stress stimuli, including cellular stress (145). Previous studies carried out in our lab have shown a significant upregulation in the quality control mechanisms (namely, ER stress and autophagy) in EAT when compared to SAT from HF patients, with and without diabetes (148). The elevated expression levels of glucose-related proteins (GRP)-78 and -94, which function as chaperone proteins and are, therefore, involved in the activation of the unfolded proteins response (UPR) or autophagy markers (such as Beclin-1, LC3-I and –II) in EAT, possibly indicate that EAT is exposed to more cellular stress (148,149) than SAT in HF patients

Therefore, to evaluate if p38 expression is different in EAT and SAT, fat explants from HF patients, with and without DM, were subjected to 10 minutes of insulin stimulation and p38 phosphorylation on Thr180/ Tyr182 residues and total p38 total expression levels were then accessed, Figure 14. The preliminary results obtained from NDM patients, Figure 14 A – G, showed that p38 Thr 180/Tyr 182 phosphorylation levels in both tissues tend to be decreased after insulin stimulation by 35,77% in SAT and by 31,98% in EAT. In fact, from the preliminary results obtained, p38 phosphorylation on Thr 180/ Tyr 182 in EAT from NDM patients, after insulin stimulation, was decreased by 31,98% when compared with basal, even after in the basal state, p38 phosphorylation on Thr 180/ Tyr 182 show an increased by 74,50%, Table 9. However, when no differences were found in p38 total expression since EAT show an increased only by 4,32%, compared to SAT, Table 9.

Table 9. Relative differences on p38 MAPK phosphorylation on Thr180/Tyr182 and total p38 MAPK expression from NDM patients.

	SAT			EAT			SAT Vs EAT	
	B (Mean±SD)	I (Mean±SD)	B Vs I (%)	B (Mean±SD)	I (Mean±SD)	B Vs I (%)	B (%)	I (%)
P- p38 (n=3)	1,000±0,177	0,642±0,259	35,77%	1,745±0,833	1,118±0,691	31,98%	74,50%	84,80%
Total p38 (n=3)	1,25±0,665			1,304± 0,632			4,32%	

B: basal; I: insulin stimulated. Relative differences in p38 MAPK phosphorylation on Thr180/Tyr182in SAT and EAT from NDM patients were calculated considering the basal from each tissue as 100%; Relative differences in the insulin effect in SAT *versus* EAT from NDM

patients was calculated considering SAT with insulin stimulation as 100%; Relative differences on total p38 MAPK expression was calculated, considering SAT as 100%.

On Figure 14 K, EAT and SAT from either NDM and DM patients were compared, DM patients show a slight decrease on p38 Thr180/Tyr182 phosphorylation levels when EAT was treated with insulin by 30,47% compared to NDM, Table 10; however, in SAT treated with insulin, the results show an increased p38 Thr180/Tyr182 phosphorylation by 47,31% in DM, compared to NDM patients, Table 10. When the total protein expression of p38 in EAT and SAT were compared either in NDM and DM patients, no differences were found in the same tissue, Table 10; however, p38 expression on DM patients tend to be approximately 50% decreased in both tissues, when compared to NDM patients, Table 10. Quantification of phosphorylated and total MAPK, as well as phospho-MAPK/Total MAPK ratio are shown on Figure 14 A-J. Due to the low number of patients used in this study, the results presented are preliminary and more studies are need.

Table 10. Relative differences on p38 MAPK phosphorylation on Thr180/Tyr182 and total p38 MAPK expression from NDM and DM patients.

	NDM SAT			**NDM SAT Vs DM SAT (%)**		**NDM EAT**			**NDM SAT Vs EAT**		**NDM EAT Vs DM EAT (%)**	
	B (Mean±SD)	I (Mean±SD)	B Vs I (%)	B (%)	I (%)	B (Mean±SD)	I (Mean±SD)	B Vs I (%)	B (%)	I (%)	B (%)	I (%)
P-p38 (n=1)	1,000	0,431	56,92%			0,898	0,744	17,14 %	10,2%	72,69 %		
Total p38 (n=2)	0,826±0,245					0,717±0,233			13,18%			
	DM SAT					**DM EAT**			**DM SAT Vs EAT**			
	B (Mean±SD)	I (Mean±SD)	B Vs I (%)	B (%)	I (%)	B (Mean±SD)	I (Mean±SD)	B Vs I (%)	B (%)	I (%)	B (%)	I (%)
P-p38 (n=1)	0,362	1,155	219,06 %	63,8%	47,31 %	O,395	0,512	31,10 %	9,11%	55,22 %	56,01 %	30,47 %
Total p38 (n=2)	O,442±0,210					0,352±0,005			20,44%		50,92%	

B: basal; I: insulin stimulated. Relative differences in p38 MAPK phosphorylation on Thr180/Tyr182 in SAT and EAT from either NDM and DM patients were calculated considering the basal from each tissue as 100%, respectively from NDM and DM patients; Relative differences in SAT versus EAT from NDM patients was calculated considering SAT from NDM, patients with insulin stimulation, as 100%, in DM patients SAT from DM, with insulin stimulation was considered as 100%; Relative differences on total p38 MAPK expression was calculated, considering SAT as 100%.

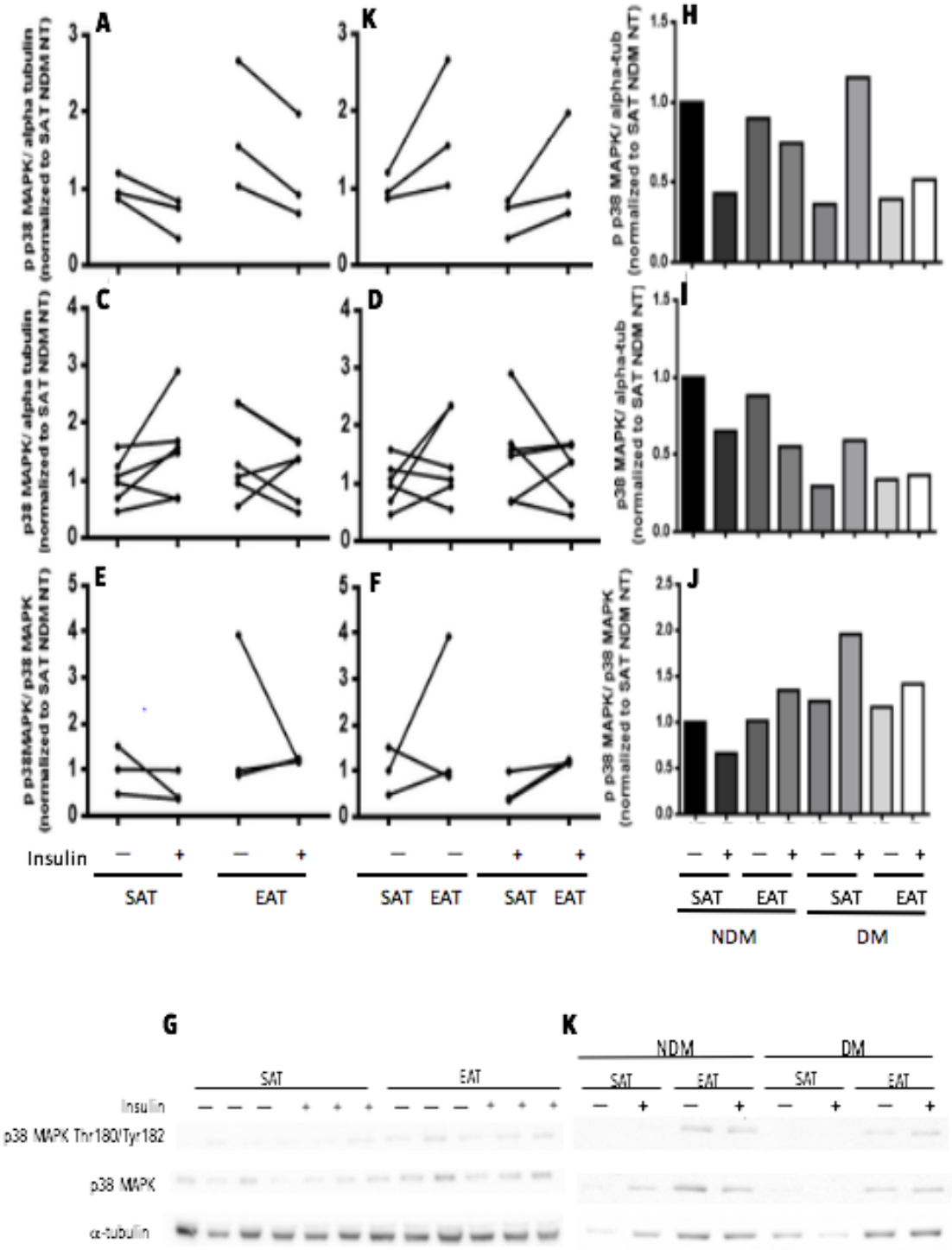

Figure 14. p38 MAPK content and phosphorylation levels in EAT and SAT from HF patients, with and without DM. 30μg of protein obtained from tissue explants from NDM patients **(G)** and NDM *versus* DM patients **(K)** was subjected to SDS-PAGE, transferred to a PDVF membrane and then to WB. EAT and SAT specific relative differences, with and without insulin stimulation, on phosphorylation level of p38 MAPK (Thr180/Tyr182) (n=3) and total p38 MAPK protein level (n=6) in NDM **(G)** and in NDM versus DM patient phosphorylation level on phosphorylation level of p38 MAPK (Thr180/Tyr182) (n=3) and total p38 MAPK protein level (n=2) were studied **(K)**. Signal quantification from total and phosphorylated p38 MAPK (Thr180/Tyr182) in NDM **(A, B, C, D, E, F)** and in NDM *versus* DM (H, I, J) Ser 473 were obtained using FIJI program, and values were corrected by normalization with α-tubulin and to the control (SAT from NDM patients without insulin stimulation). Results were presented as mean on line graphs.

It is known that EAT works as a metabolic buffer, protecting heart and coronaries arteries, it is also responsible for cardiac calcium homeostasis and energy supply. Therefore, EAT can be metabolically more active when compared to SAT, in order to provide fatty acids as a cardiomyocyte substrate supply. The cardiomyocyte is a cell that needs permanent energy supply, since it is working continually contrasting with skeletal myocytes. In order to study this hypothesis, the expression level of fatty acid synthase (FAS) were accessed in EAT and SAT from NDM patients, Figure 15. FAS represents a catalytic enzyme that promotes the palmitate synthesis, from acetyl-CoA and malonyl-CoA, in the presence of NADPH (150). Palmitate is one of the fatty acids that it is used as an energy substrate for cardiomyocytes (151). The preliminary results obtained indicate an increased expression in FAS, by 34,30% in EAT when compared with SAT, Table 11 and Figure 15 A and B.

More studies need to be performed in a larger number of tissue samples in order to obtain conclusive results, regarding both protein expression, as well as phosphorylation status.

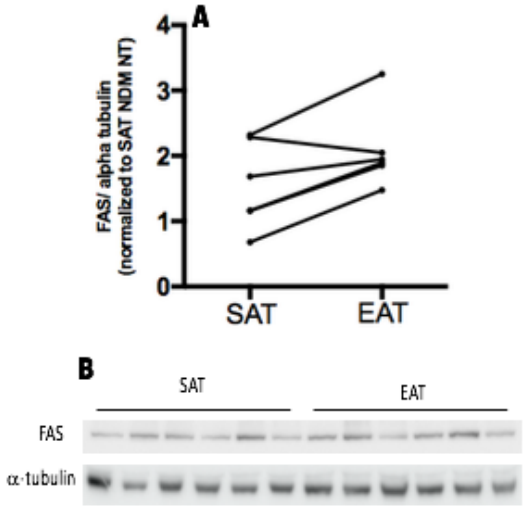

Figure 15. FAS expression in EAT and SAT. 30μg of protein obtained from tissue explants from NDM patients was subjected to SDS-PAGE, transferred to a PDVF membrane and then to WB. EAT and SAT specific relative differences FAS (n=3) in NDM (C). Signal quantification from FAS (A, B) was obtained using FIJI program, and values were corrected by normalization with α-tubulin and to the control (SAT from NDM patients without insulin stimulation).

Table 11. Relative differences in total FAS expression from NDM patients.

	SAT	EAT	SAT Vs EAT
Total FAS	1,548±0,665	2,079±0,606	34,30%

Relative differences on total FAS expression on NDM patients, was calculated, considering SAT as 100%.

3.3Mitochondrial respiration in EAT and SAT from HF patients

Recent preliminary data from our manuscript in preparation show that there is increased mitochondrial respiration in EAT when compared with SAT from HF patients (152). EAT is considered as a beige fat tissue, with both WAT and BAT-related features, including high UCP1 expression levels. On the other hand, the differences observed between EAT and SAT disappeared when respiration was measured under the presence of GDP, a UCP1 inhibitor, Figure 16.

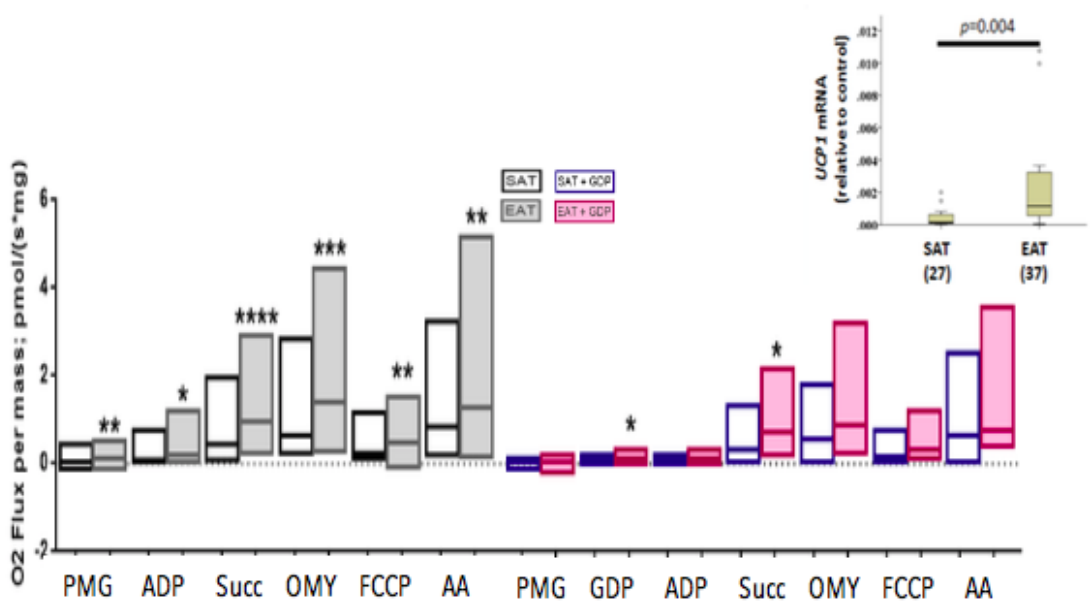

Figure 16. Mitochondrial respiration in NDM (n=40) **and DM** (n=26) **subjects, measured through high resolution respirometry in the absence of GDP,** SAT (n=49) versus EAT (n=49**) (gray) and in the presence of GDP**, SAT (n=17) versus EAT (n=17) **(pink) (UCP1 inhibition).** Results were normalized per mg of tissue. PMG: pyruvate, malate and glutamate; GDP: Guanosine diphosphate; ADP: Adenosine diphosphate; Succ: succinate; Omy: oligomycin; FCCP: trifluoromethoxy carbonylcyanide phenylhydrazone; AA: antimycin A.

These results might elucidate about the UCP1 relevance in EAT mitochondrial activity and metabolism, leading to heat production and consequently a protective effect on heart by preventing hypothermia. However, our previously studied protocol, Figure 17, shows the contribution of each mitochondrial complex to mitochondrial respiration and the OXPHOS state after addition and NADH- and S-pathway linked substrates, but no contribution of fatty acid oxidation was evaluated.

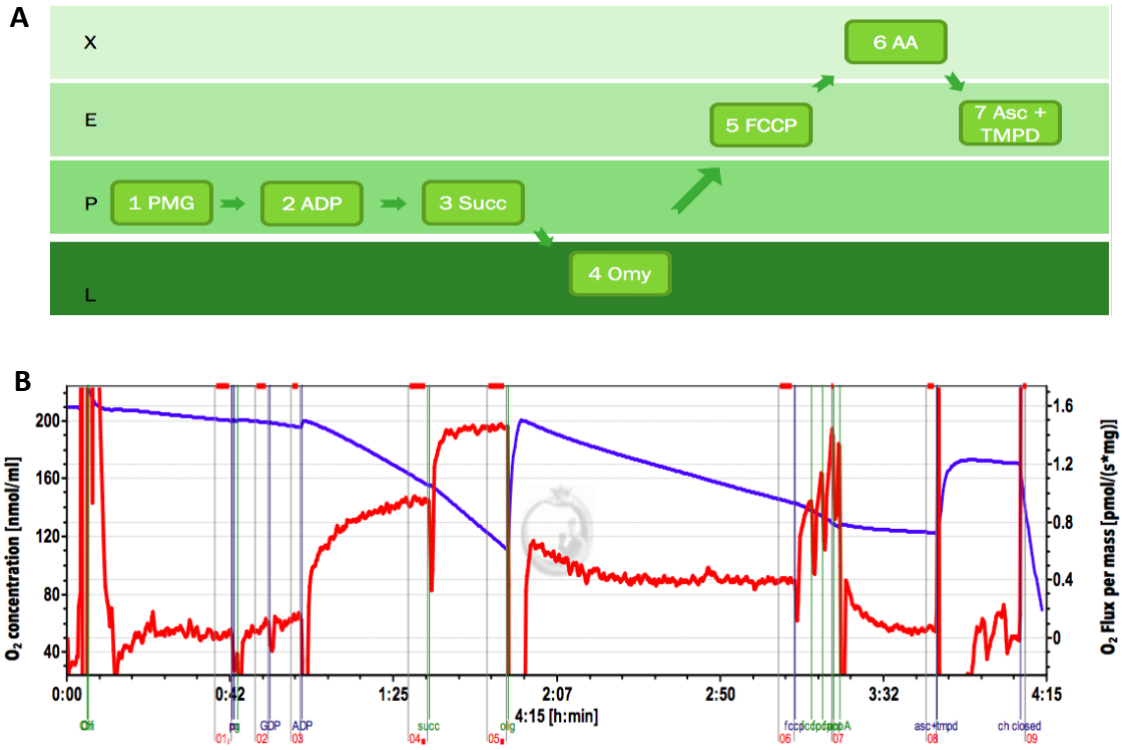

Figure 17. Schematic representation of the protocol used in the previous studies (A) and a representative trace of mitochondrial respiration in EAT (B). PMG: pyruvate, malate and glutamate; GDP: Guanosine diphosphate; ADP: Adenosine diphosphate; Succ: succinate; Omy: oligomycin; FCCP: trifluoromethoxy carbonylcyanide phenylhydrazone; AA: antimycin A; Asc+TMPD: ascorbate and tetramehyl-p-phenylenediamine. L, P, E, X indicate the specific mitochondrial respiratory states: LEAK (L), OXPHOS respiration (P); ET-pathway respiration (E) and X (residual oxygen respiration).

Since our preliminary results of FAS expression appears to be increased in EAT when compared with SAT, a different reference protocol (RP) 2 (136) was used during these studies, in order to measure also the contribution of β-oxidation for mitochondrial respiration, Figure 18.

Figure 18. Reference Protocol 2. Schematic representation of the RP2 protocol additions **(A)** and representative experimental traces on an RP2 protocol run **(B)**. Dig: Digitonin: GDP: Guanosine diphosphate; ADP: Adenosine diphosphate, Mal.1: Malate; Oct: octanoylcarnitine, PMG: pyruvate, malate and glutamate; Succ: succinate; CCCP: Carbonyl cyanide 3-chlorophenyl hydrazone; Rot: rotenone, AA: antimycin A; Asc+TMPD: ascorbate and tetramehyl-p-phenylenediamine. P, E, X indicate the specific mitochondrial respiratory states: OXPHOS respiration (P); ET-pathway respiration (E) and X (residual oxygen respiration).

By using the RP2 suit protocol, it is possible to evaluate the contribution of FA oxidation or the F-pathway, in the addition to the NADPH N- and S- pathways contributions to the overall OXPHOS in these tissues. Thus, the various substrates, uncoupler and inhibitors shown on Figure 18 A, allowed us to evaluate the specific mitochondrial respiratory states: OXPHOS respiration (P), Electron transference pathway respiration (ET) and the residual oxygen consumption (ROX). A representative experimental trace of EAT mitochondrial oxygen consumption is shown on Figure 18 B.

The data referent to the mitochondrial oxygen consumption rate was calculated regarding the oxygen consumption rate per wet weight per tissue, (pmol O_2 s^{-1} mg^{-1}), as shown in the figure traces. Data were normalized to the COX activity values obtained per experiment. The addition of Asc + TMPD represents the last step on RP2, measuring complex IV activity in the Electron transfer. COX represents one of the biomarkers used for mitochondrial content normalization (153). Data was presented as the median and the moderate outliers are shown as circles in box-and-whisker plots in the figures related

with mitochondrial respiration and lie more than one and a half times the interquartile range (IQR), that is, below Q_1 - 1.5 X IQR or above Q_3 + 1.5 X IQR.

When mitochondrial respiration rates were evaluated in regard to the tissue type from NDM patients, in the absence of any additions, EAT presented increased residual oxygen consumption (ROX) when compared with SAT (median: EAT=0,029 *versus* SAT=0,002, p value= 0,043), even without any substrate addition, Figure 19. In fig 18 ROX is before GDP. To evaluate if UCP1 could influence mitochondrial activity in EAT, both fat depots, from either NDM and DM patients, were treated with GDP (an UCP1 inhibitor), at the start of the experiments, followed by the addition of ADP for the depletion of endogenous substrates, already at this stage EAT presents increased respiration compared to SAT (median: EAT=0,021 *versus* SAT=0,009; p value=0,010). Subsequently, EAT exhibits increased OXPHOS mediated by the contribution of both fatty acid oxidation and the N pathway, by addiction of Mal.1 (median: EAT=0,051 *versus* SAT=0,017; p value=0,022) and Oct (median: EAT=0,048 *versus* SAT= 0,023; p value=0,022), respectively, Figure 19. However, no differences were found when F(N)-linked respiration ratio were evaluated, Figure 20 C.

Following Oct, addiction of PMG supports the OXPHOS mediated by NADPH-pathway malate, glutamate as well as pyruvate to support FN-OXPHOS, by complex I energization in addition to the F-pathway. After PMG addiction no differences were found between the two tissues; however, EAT shows a tendency for an increased PMG-induced respiration when compared to SAT (median: EAT=0,060 *versus* SAT=0,035; p value=0,053). Though, no differences were found in complex I respiratory ratio between the two tissues, Figure 20 A.

When complex II was energized by succinate addition no further significant increase in OXPHOS was observed. The complex II respiration ratio was not different between the two fat tissues, Figure 20 B. The subsequent titration of the uncoupler CCCP, promoted the experimentally induce noncoupled state of maximum respiration, CCCP disrupts the proton gradient across the inner membrane promoting the measurement of the maximal capacity of the electron transfer pathway, which promotes the highest oxygen consumption rates. Uncoupled EAT maximum respiration shows a tendency for an

increase noncoupled state of maximum respiration when compared to SAT (median: EAT=0,13 *versus* SAT=0,12; p value=0,053), Figure 19. In the last steps of this RP2 respiration protocol, complex I and complex II were inhibited by rotenone and antimycin A, respectively, Figure 19. Either evaluation of mitochondrial respiration after complex I or complex II inhibition was not different in either tissue, Figure 19. These respiratory ratios are only relative representations of each step in the process. The overall OXPHOS in tissues is best represented as a whole as shown in Figure 19.

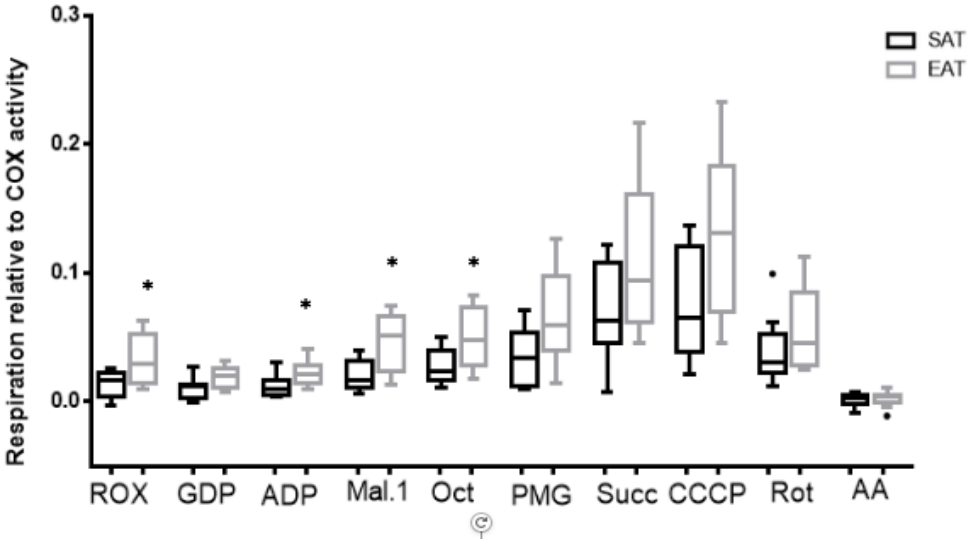

Figure 20. Mitochondrial respiration in NDM subjects, measured through high resolution respirometry in the presence of GDP (UCP1 inhibition), SAT (n=9) *versus* EAT (n=10). Results were normalized by COX activity. Data are medians and moderate outliers, shown as circles in box-and-whisker plots, lie more than one and a half times the interquartile range (IQR), that is, below Q_1 - 1.5 X IQR or above Q_3 + 1.5 X IQR. Mann-Whitney U test was applied and p<0,05 was considered significant. p values [NDM in the presence of GDP]: ROX p value= 0,043); ADP (p value=0,010); Mal.1 (p value=0,022); Oct (p value=0,022).

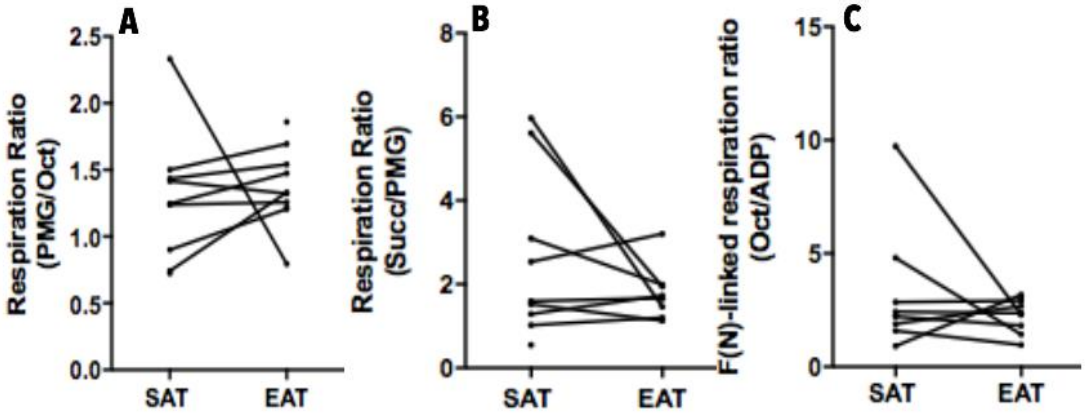

Figure 19. Mitochondrial complex analysis in NDM subjects, measured through high resolution respirometry in the presence of GDP (UCP1 inhibition) (D-E), SAT (n=9) *versus* EAT (n=10). **Complex I Respiration Control Ratio (PMG/Oct) (A), Complex II Respiration Control Ratio (Succ/PMG) (B) and F(N)-linked respiration Ratio (Oct/ADP) (C).** Mann-Whitney U test was applied and p<0,05 was considered significant.

When mitochondrial respiration was evaluated in SAT and EAT from DM patients with HF, with UCP1 inhibition by GDP, no significant differences were observed, Figure 21, and no differences were observed in the respiration ratios either, Figure 22.

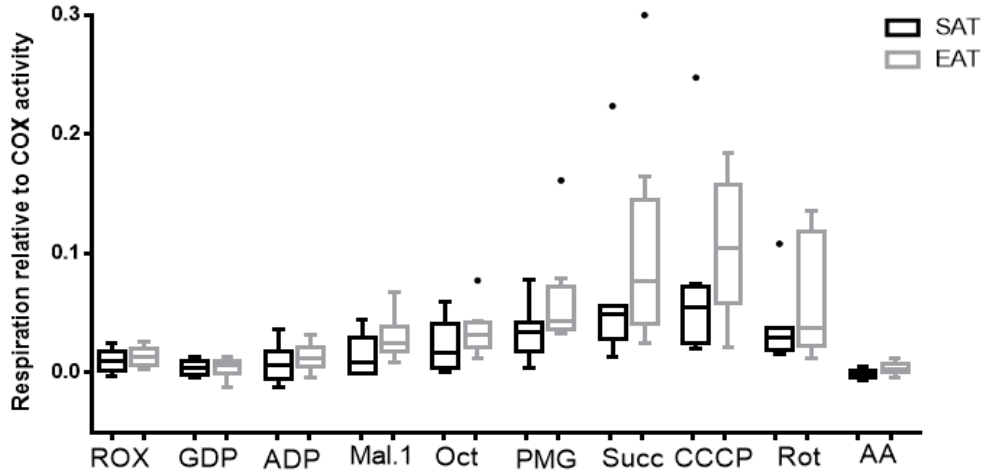

Figure 21. Mitochondrial respiration in DM patients, measured through high resolution respirometry in the presence of GDP (UCP1 inhibition), SAT (n=8) *versus* EAT (n=9). Results were normalized by COX activity. Data are medians and moderate outliers, shown as circles in box-and-whisker plots, lie more than one and a half times the interquartile range (IQR), that is, below Q_1 - 1.5 X IQR or above Q_3 + 1.5 X IQR. Mann-Whitney U test was applied and p<0,05 was considered significant.

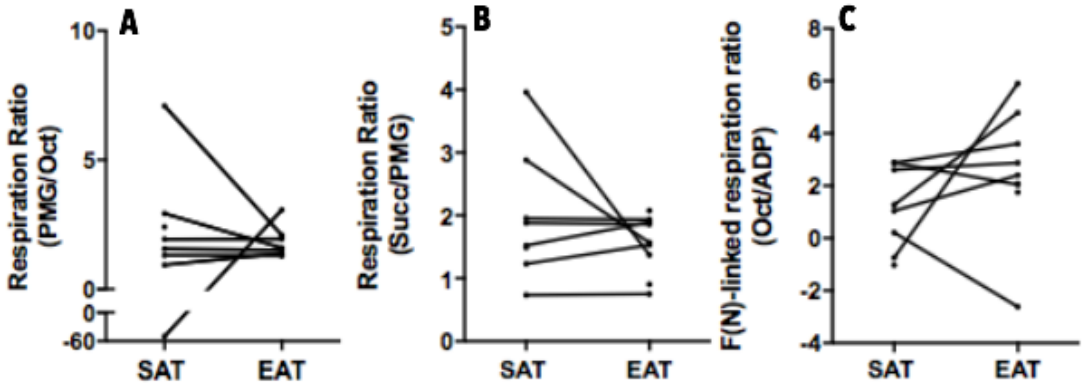

Figure 22. Mitochondrial complex analysis in DM patients, measured through high resolution respirometry in the presence of GDP (UCP1 inhibition), SAT (n=8) *versus* EAT (n=9). **Complex I Respiration Control Ratio (PMG/Oct) (A), Complex II Respiration Control Ratio (Succ/PMG) (B) and F(N)-linked respiration Ratio (Oct/ADP) (C).** Mann-Whitney U test was applied and p<0,05 was considered significant**.**

When both tissue results were combined and the only variable evaluated was the presence or absence of diabetes (NDM and DM) in the presence of GDP, no significant differences were found, except in the ROX state, before addition of any substrate (median: NDM (SAT + EAT)=0,017 *versus* DM (SAT + EAT)=0,012; p value=0,010) and after GDP addition (median: NDM (SAT + EAT)=0,013 *versus* NDM (SAT + EAT)=0,005; p value < 0,001), Figure 23. No differences were found when complex I and II activity or F(N)-linked respiration were evaluated when comparing NDM *versus* DM patients Figure 24.

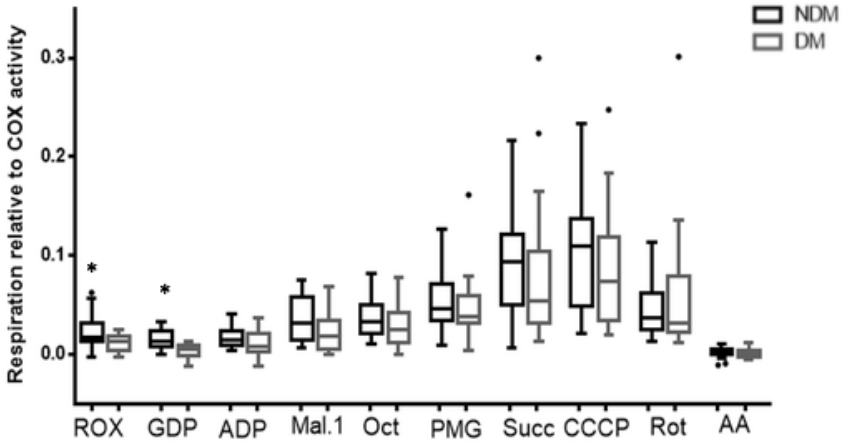

Figure 23. Mitochondrial respiration in NDM (n = 19, SAT n=9 + EAT = 10) **and DM** (n=10, SAT n=8 + EAT = 9) **patients, measured through high resolution respirometry in the presence of UCP1 inhibition (GDP addition).** Results were normalized by COX activity. Data are medians and moderate outliers, shown as circles in box-and-whisker plots, lie more than one and a half times the interquartile range (IQR), that is, below Q_1 - 1.5 X IQR or above Q_3 + 1.5 X IQR. Mann-Whitney U test was applied and p<0,05 was considered significant. p values: ROX (p value=0,010); GDP (p value < 0,001).

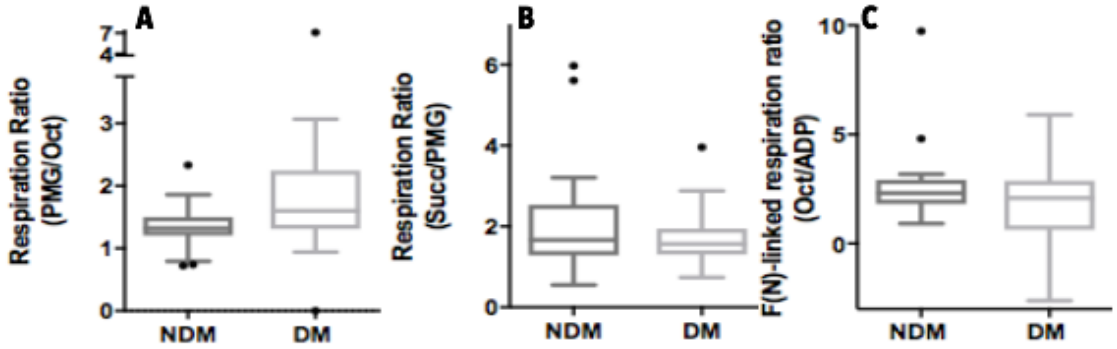

Figure 24. Mitochondrial complex analysis in NDM (n = 19, SAT n=9 + EAT = 10) **and DM** (n=10, SAT n=8 + EAT = 9) **patients, measured through high resolution respirometry in the presence of GDP (UCP1 inhibition) Complex I Respiration Control Ratio (PMG/Oct) (A), Complex II Respiration Control Ratio (Succ/PMG) (B) and F(N)-linked respiration Ratio (Oct/ADP) (C).** Data are medians and moderate outliers, shown as circles in box-and-whisker plots, lie more than one and a half times the interquartile range (IQR), that is, below Q_1 - 1.5 X IQR or above Q_3 + 1.5 X IQR. Mann-Whitney U test was applied and p<0,05 was considered significant.

Furthermore, mitochondrial respiration was evaluated comparing only the two fat tissue types, thus EAT from both NDM and DM were compared with SAT from both NDM and NDM, Figure 25. EAT presents increased ROX respiration when compared with SAT (median: EAT (NDM + DM)=0,017 *versus* SAT (NDM + DM)=0,014; p value=0,013), Figure 25. Moreover, EAT exhibits a significant increase in OXPHOS mediated by fatty acid oxidation with contribution from the N-pathway, by addition of Mal.1 (median: EAT (NDM + DM)=0,031 SAT (NDM + DM)=0,014; p value=0,002) and Oct (median: EAT (NDM + DM)=0,039 *versus* SAT (NDM + DM)=0,021; p value=0,013), respectively, Figure 25. However, no differences were found when F(N)-linked respiration rate was calculated as the ratio between Oct/ADP, Figure 26 C.

Moreover, after the addiction of PMG, energizing complex I and further contributing to the N-pathway, EAT exhibits a further and significant increase in respiration when compared to SAT (median: EAT (NDM + DM)=0,054 *versus* SAT (NDM + DM)=0,035; p value=0.010), Figure 25. However, the complex I respiration ratio do not shown any differences between the two tissues, Figure 26 A. When complex II was energized by succinate addition further contributing to OXPHOS, no differences were found, Figure 25. The complex II respiration ratio was not different in the two fat tissues, Figure 26 B. Furthermore, titration of CCCP, to promote the noncoupled state of maximum respiration, induced a significant increase in the EAT noncoupled state of maximum respiration when compared to SAT (median: EAT (NDM + DM)=0,104 *versus* SAT (NDM + DM)=0,062; p value=0,047). Finally, complex I and complex II inhibition by rotenone and antimycin A addiction, respectively, did not show significant differences in either the two fat tissues.

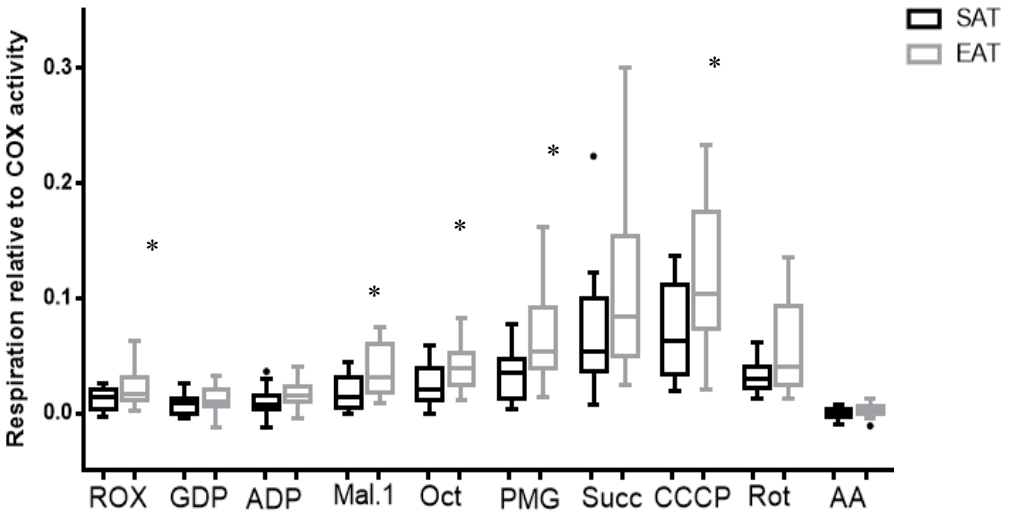

Figure 25. Mitochondrial respiration in SAT (n = 17, NDM n=9 + DM = 8) **and EAT** (n=19, NDM n=10+ DM n=9), **measured through high resolution respirometry with UCP1 inhibition (GDP addition).** Results were normalized by COX activity. Data are medians and moderate outliers, shown as circles in box-and-whisker plots, lie more than one and a half times the interquartile range (IQR), that is, below Q_1 - 1.5 X IQR or above Q_3 + 1.5 X IQR. Mann-Whitney U test was applied and p<0,05 was considered significant. p values: ROX (p value=0,013); Mal.1 (p value=0,002); Oct (p value=0,013), PMG (p value=0,010), CCCP (p value=0,047).

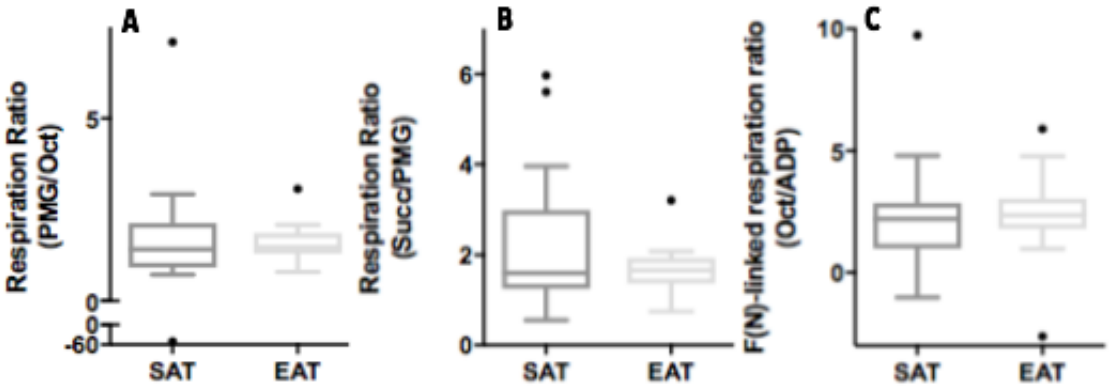

Figure 26. Mitochondrial complex analysis in SAT (n = 17, NDM n=9 + DM = 8) **and EAT** (n=19, NDM n=10+ DM n=9)**, measured through high resolution respirometry in the presence of GDP (UCP1 inhibition). Complex I Respiration Control Ratio (PMG/Oct) (A), Complex II Respiration Control Ratio (Succ/PMG) (B) and F(N)-linked respiration Ratio (Oct/ADP) (C).** Data are medians and moderate outliers, shown as circles in box-and-whisker plots, lie more than one and a half times the interquartile range (IQR), that is, below Q_1 - 1.5 X IQR or above Q_3 + 1.5 X IQR. Mann-Whitney U test was applied and p<0,05 was considered significant.

It is really important to note that EAT presents a significantly increased β oxidation in comparison with SAT even after UCP1 inhibition. This observation is abolished when the respiration of both tissues is combined and all we evaluate is disease status. On the other hand, and as mentioned previously, results from our previous studies (152) when we evaluated only the effect of NADH- and S- linked OXPHOS without the contribution

of the F-pathways, EAT respiration was significantly increased only in the absence of UCP-1 inhibition (GDP) compared to SAT, while in the presence of UCP-1 inhibition this significance disappeared.

Chapter 4. Discussion and Conclusions

Nowadays, CVD represents one of the most lethal complications related with the development of DM (21,22). EAT, due its straight cross-talk between the epicardial adipocytes and the cardiomyocytes (58), has been associated with the development of these complications (53). Therefore, the purpose of this study was to evaluate differences on protein phosphorylation levels in EAT and SAT, with and without insulin stimulation and the protein expression of a few important nodes in metabolism, as well as alterations on mitochondrial respiratory in either tissue, from HF patients, with and without diabetes.

Insulin is a peptide hormone that is secreted by the pancreatic β-cells with a wide range of functions in insulin sensitive tissues, in order to maintain whole body homeostasis (154). Indeed, insulin stimulation can affect several pathways, regarding the type of tissue associated. However, this stimulation involves the activation of innumerous downstream protein kinases by phosphorylation, leading to insulin signaling and consequently stimulation of its particular functions in metabolism. In adipose tissue, insulin stimulation is important in glucose uptake, lipogenesis and lipid storage (154).

AKT/PKB is a center downstream protein kinase in the insulin cascade and works as an intermediate on most of the insulin-stimulated functions (154). Our preliminary results, from NDM patients, shown for the first time, increased content in AKT/PKB in EAT when compared to SAT, Figure 12. Moreover, AKT/PKB phosphorylation on Ser 473 is increased in EAT compared to SAT, either in NDM and DM patients, although in DM patients this increase is subtler. Few studies have been developed on EAT metabolic characterization, and until now, no studies have shown the insulin effects on EAT. Moreover, the decreased AKT phosphorylation on DM patients, can be related with the decrease in insulin sensitivity that leads to the development of insulin resistance (154). Although insulin resistance can also be a consequence of obesity, no differences were found regarding BMI from NDM and DM patients, Table (6,7).

AKT/PKB phosphorylation induces glucose uptake by increased GLUT4 translocation (155). Although, previous studies carried out in our lab reported a decreased glucose uptake, lipolysis and lipid storage capacity in EAT adipocytes when

compared to SAT adipocytes, in part because these cells are much smaller then SAT adipocytes, but there are many more cells per mg tissue in EAT compared to SAT (80,140). The smaller EAT adipocyte size, related with the decreased lipid storage can be a protective response against increased lipid accumulation, lipotoxicity (140). No differences were found in MAPK (ERK 1/2) total expression and MAPK phosphorylation on Thr202/Tyr204 in SAT and EAT from either NDM and DM patients, Figure 13. However, an increased phosphorylation of MAPK protein after insulin stimuli, might elucidate if the differences on adipocyte size might alter the whole tissue metabolism, being the EAT adipocytes more metabolic active than SAT adipocytes. Insulin stimuli, trough MAPK modulates protein synthesis (156) as well as adipocyte differentiation (156). In fact, MAPK phosphorylation is related with the increased lipolysis rate (157,158) , which was also demonstrated as decreased in EAT adipocytes when compared to SAT (80). Although the results presented are only preliminary and not conclusive, due to the low number of experiences and more patients needed to be compared.

From the same family than MAPK there are more proteins that are also activated under insulin stimuli. Indeed, the MAPK family of proteins can influence either physiological and pathological conditions, once p38 and c-Jun N-terminal kinases (JNK) are activated in the presence of stress and in the last recourses can induce autophagy or cell apoptosis in several tissues (147). Although, metabolic syndrome, present in diabetic patients and obese subjects, is associated with increased cellular stress, no differences were shown in EAT and SAT from NDM and DM patients, Figure 14. In accordance with previous studies, shown no differences in autophagy markers as Beclin-1, LC3-I and –II (148), our results shown a tendency for a decreased p38 MAPK phosphorylation in 180/182 residues in DM patients when compared with NDM. More samples need to be compared in order to obtain more solid and robust results.

Cardiomyocytes represent one of the most demanding cells in terms of homeostasis and energy, their involuntary contractility, responsible for blood pumping, leads to a higher energetic need. The close anatomical relation between EAT and cardiomyocytes suggests a higher cross-talk and EAT seems to be directly related with FA supply to the cardiomyocytes. Indeed, our results shown an increased FAS expression in EAT when

compared to SAT, Figure 15. FAS is a catalytic enzyme responsible for the synthesis of palmitate, (150), a fatty acids that it is used as an energy substrate for cardiomyocytes (151).

EAT comprises both WAT and BAT features (126). BAT is more related with mitochondrial function, since there is an increased number of mitochondria in this tissue, which has as its main function is to perform cardiac thermogenesis (40,42). However, and contrary to the idea that WAT is merely a tissue of fat deposition, this type of fat tissue can also function as a metabolic organ, contributing for all body homeostasis (37,44). Indeed, mitochondrial dysregulation in WAT is related with the development of DM (159). EAT also expresses UCP1, a protein considered as a biomarker for BAT, responsible for heat production; in addition, EAT has also increased content in other mitochondrial-related proteins, as PGC-1α and PRDM16 (102,126). UCP1 works as an uncoupler, increasing the higher rate of inner membrane proton conductance, needed to uncouple OXPHOS from ATP synthesis (102,160), and the energy is dissipated in the form of heat. In fact, in patients with coronary atherosclerosis there are increased expression of these BAT-related markers in EAT (126), suggesting the importance of EAT either in the maintenance and pathological alterations of cardiomyocyte function.

Our previous results from amanuscript in preparation indicated that EAT has increased mitochondrial respiration when compared to SAT from HF patients. However, after inhibition of UCP1, by GDP, the differences between tissues were abolished, which indicates the UCP1 important activity in EAT to prevent cardiac hypothermia by heat production (152). Although, EAT is also responsible to supply cardiomyocytes' high energy demands by releasing FA (REF). However, the previous used protocol did not evaluate the influence of FA oxidation in EAT mitochondrial respiration.

Therefore, in the present study, mitochondrial respiration was accessed, both in EAT and SAT from HF patients, using the SUIT-RP2 protocol, in the presence and GDP. SUIT-RP2 protocol was designed to evaluate the contribution of fatty acid oxidation (F-pathway) on OXPHOS and electron transfer capacity; however, no LEAK respiration was evaluated using this protocol (136).

In fact, it is known that in physiological conditions, UCP1 thermogenic functions are activated by long chain fatty acids (could it be activated by OCT?), including palmitate, one of the FA used as cardiomyocytes fuel (151,161); indeed, FA and purine nucleotides, as GDP, can compete for the UCP1 binding site (162). Consequently, to evaluate only the influence of FA oxidation either in EAT and SAT, Oct was used, to prevent the competition with GDP. Oct is a saturated medium chain fatty acid (8 carbons: octanoic acid), and it is linked with carnitine to facilitate the transport into the mitochondrial matrix (136). Moreover, the results per mg in wet weight of each adipose tissue sample obtained after titration with substrates, uncoupler and inhibitors were normalized by COX activity, after Asc+TMPD, the last RP2 addiction (153).

Although human fat tissues analyzed show lower mitochondrial oxygen respiration when compared specially with human muscle (163,164), due to lower mitochondrial content, the high-resolution respirometry (HRR) technique is sensitive enough to still measure respiration (152).

This study demonstrates, for the first time, that EAT mitochondrial respiration, with F-pathway contribution, is increased when compared to SAT collected from HF patients, in the presence of GDP, an UCP1 inhibitor, after normalization by COX activity.

Using the SUIT-RP2 protocol for mitochondrial respiration measurements, ADP is added at high concentration, after tissue permeabilization with digitonin, to promote kinetic-saturation of OXPHOS capacity by depletion of the endogenous substrates present in the fat cells; thus, to evaluate GDP effect in both tissues, GDP was added before ADP.

The first value obtained with this protocol was mitochondrial oxygen residual respiration (ROX), which corresponds to the period of time ranging from the permeabilization of the tissues with digitonin to the addition of the first substrate which, in this case, is Mal.1. The early addiction of Mal.1 together with Oct is used for stimulation of F-OXPHOS with an obligatory contribution of the N-pathway (54). Therefore, ROX state include the purine nucleotide addictions of GDP and ADP, that do not contribute for energization of any complex or for F-pathway stimulation.

According to the literature, BAT shows increased basal respiration when compared to WAT in animal studies (165) as well as in human AT (152). In fact, UCP1 can be considered as responsible for the higher mitochondrial respiration rate, even in the basal state, in BAT, since UCP1 is an uncoupler protein and facilitates proton leak (160). Accordingly, in the present study, EAT from NDM patients shows an increased ROX, basal respiration before UCP1 inhibition, Figure 18.

Furthermore, after GDP addiction, we observed also an increased mitochondrial respiratory in EAT after ADP, Mal.1 and Oct addictions compared to SAT, Figure 18; these results are in accordance with the literature, since the cumulative effect of the ADP, Mal.1 and Oct was sufficient for stimulated OXPHOS mediated by FA oxidation, (F(N)-linked respiration) (136,164).

Regarding SAT, GDP inhibition did not alter mitochondrial respiration, since UCP-1 expression is diminished or inexistent in WAT, mostly present in beige and brown adipocytes (166).

On DM patients, the increased FA uptake into the cardiomyocytes as a result of increased FA in circulation is related with CVD development, including HF (80,167,168). However, our results obtained with DM patients show no effect in mitochondrial respiration under UCP1 inhibition, Figure 20. In this case, the similar mitochondrial respiration in both tissues can be a consequence of the unbalance of mitochondrial Ca^{2+} homeostasis, leading to Ca^{2+} current alterations and, consequently, cardiomyocyte contractibility dysfunction, promoted by alterations on insulin resistance (127,128).

Despite the study population presenting some form of HF, NDM patients show increased residual mitochondrial respiration compared with DM patients (Figure 21), which may reflect basal mitochondrial dysfunction in the diabetic state (166). OXPHOS can not be measured in fat tissues of healthy subjects.

When mitochondrial respiration was assessed in both tissues, regardless of the presence or absence of DM, increased residual mitochondrial respiration, as well as increase in respiratory mitochondrial measurements after Mal.1, Oct, PMG and CCCP were observed in EAT, Figure 24. In relation to the observed increased mitochondrial

respiration after PMG addiction, this could indicate an increased response on OXPHOS by N and F-pathway stimulation. The present results, together with our manuscript in preparation, are the first studies to be reported regarding mitochondrial respiration in EAT from subjects subjected to heart surgery due to HF.

Besides EAT mitochondrial respiration, expression of insulin signaling related proteins were also evaluates; however, due the small n, no solid conclusions can be taken.

In the presented study, mitochondrial respiration results, data were normalized by COX activity values, although it is considered a valid biomarker used for mitochondrial content normalization (153), the confirmation of these values by mitochondrial DNA should also be considered. Moreover, a pilot study where EAT is tested using the SUIT-RP2, in the presence of a long chain fatty acid (i.e. palmytoycarnitine) and UCP1 inhibition by GDP, in order to further confirm if the chain length can influence EAT F-pathway contribution on OXPHOS, in a different way than Oct (a medium-chain fatty acid).

The presented study was entirely developed with human biopsies collected from living patients undergoing cardiac surgery, therefore the EAT and SAT sample size did not allow to perform all experiments in the same sample. Indeed, after tissue collection, subject groups were put together and the specific characteristics from each patient, specially the presence or absence of diabetes, but also the BMI, sex, and type of cardiac disease were identified. In the present study, our population was only divided regarding presence of absence of DM. Moreover, we are unable to collect EAT biopsies from healthy subjects to compare with the presented results.

In conclusion, although the presented results are preliminary, we have shown an increase in respiration after Mal.1, Oct, PMG and CCCP additions, which confirms the contribution of F-pathway and β-oxidation as an important source of energy for EAT and thus its increased mitochondrial respiration in the presence of GDP, an UCP1 inhibitor, after normalization by COX activity, when compared to SAT. In fact, as our study population is constituted from HF patients, the increase in EAT mitochondrial respiration might be specific of the tissue or might related with the cardiac progression, we would

only be able to distinguish this after evaluation of healthy tissue, therefore we compare tissues in the same subjects, rather than healthy and unhealthy subjects. Due to the anatomical relation between EAT and the heart, EAT characterization might contribute for the discovery of early biomarkers for potential therapeutic targets, in cardiac disease.

Chapter 5. References

1. American Diabetes Association. Diagnosis and classification of diabetes mellitus.

Diabetes Care. 2014;37(SUPPL.1):81–90.

2. IDF International Diabetes Federation. IDF Diabetes Atlas, 7th edn. Brussels B, Federation ID. DIABETES. 2015.

3. SPD. Factos e Numeros. 2016.

4. Borchers AT, Uibo R, Gershwin ME. The geoepidemiology of type 1 diabetes. Autoimmun Rev. 2010;9:A355–65.

5. Butalia S, Kaplan GG, Khokhar B, Rabi DM. Environmental Risk Factors and Type 1 Diabetes: Past, Present, and Future. Can J Diabetes. 2016;40(6):586–93.

6. Jin W, Patti M-E. Genetic determinants and molecular pathways in the pathogenesis of Type 2 diabetes. Clin Sci. 2009;116(2):99–111.

7. Olefsky JM, Kolterman OG. Mechanisms of insulin resistance in obesity and noninsulin-dependent (type II) diabetes. Am J Med. 1981;70(1):151–68.

8. Carvalho E, Jansson P, Axelsen M, Eriksson JW, Huang X, Groop L, et al. Low cellular IRS 1 gene and protein expression predict insulin resistance and NIDDM. FASEB J. 1999;13(15):2173–8.

9. Carvalho E, Jansson PA, Nagaev I, Wenthzel AM, Smith U. Insulin resistance with low cellular IRS-1 expression is also associated with low GLUT4 expression and impaired insulin-stimulated glucose transport. FASEB J. 2001;15(6):1101–3.

10. Rondinone CM, Carvalho E, Wesslau C, Smith UP. Impaired glucose transport and protein kinase B activation by insulin, but not okadaic acid, in adipocytes from subjects with Type II diabetes mellitus. Diabetologia. 1999;42(7):819–25.

11. Carvalho E, Eliasson B, Wesslau C, Smith U. Impaired phosphorylation and insulin-stimulated translocation to the plasma membrane of protein kinase B/Akt in adipocytes from type II diabetic subjects. Diabetologia. 2000;43(9):1107–15.

12. Artunc F, Schleicher E, Weigert C, Fritsche A, Stefan N, Haring H-U. The impact of insulin resistance on the kidney and vasculature. Nat Rev Nephrol. 2016;12:721–37.

13. Kahn SE, Hull RL, Utzschneider KM. Mechanisms linking obesity to insulin resistance and type 2 diabetes. Nature. 2006;444:840–6.

14. Bergman RN, Ader M. Free Fatty Acids and Pathogenesis of Type 2 Diabetes Mellitus. Trends Endocrinol Metab. 2000;11(9):351–6.

15. Moller DE, Kaufman KD. Metabolic Syndrome: A Clinical and Molecular Perspective. Annu Rev Med. 2005;56(1):45–62.

16. Fowler MJ. Microvascular and Macrovascular Complications of Diabetes. Clin Diabetes. 2011;29(3):116–22.

17. Bansal V, Kalita J, Misra UK. Diabetic neuropathy. Postgrad Med J. 2006;82:95–

100.

18. Cao Z, Cooper ME. Pathogenesis of diabetic nephropathy. J Diabetes Investig. 2011;2(4):243–7.

19. Wong TY, Cheung CMG, Larsen M, Sharma S, Simó R. Diabetic retinopathy. 2016;2:16030.

20. Hashkes, Philip J., Laxer RM. Paneni F, Beckman JA, Creager MA, Cosentino F. Diabetes and vascular disease: Pathophysiology, clinical consequences, and medical therapy: Part i. European Heart Journal. 2013. p. 2436–46. Jama. 2014;305(15):1591–2.

21. Cavan D, Harding J, Linnenkamp U, Makaroff L, Magliano D, Ogurtsova K, et al. Diabetes and Cardiovascular Disease. 2016. 144 p.

22. Laing SP, Swerdlow AJ, Slater SD, Burden AC, Morris A, Waugh NR, et al. Mortality from heart disease in a cohort of 23,000 patients with insulin-treated diabetes. Diabetologia. 2003;46(6):760–5.

23. Martín-Timón I. Type 2 diabetes and cardiovascular disease: Have all risk factors the same strength? World J Diabetes. 2014;5(4):444.

24. Fox KAA, Després JP, Richard AJ, Brette S, Deanfield JE. Does abdominal obesity have a similar impact on cardiovascular disease and diabetes? A study of 91 246 ambulant patients in 27 European Countries. Eur Heart J. 2009;30(24):3055–63.

25. Tuttolomondo A, Maida C, Maugeri R, Iacopino G, Pinto A. Relationship between diabetes and ischemic stroke: Analysis of diabetes-related risk factors for stroke and of specific patterns of stroke associated with diabetes mellitus. Diabetes Metab J. 2015;6(5).

26. Marso SP, Hiatt WR. Peripheral Arterial Disease in Patients With Diabetes. J Am Coll Cardiol. 2006;47(5):921–9.

27. Leon BM, Maddox TM. Diabetes and cardiovascular disease: Epidemiology, biological mechanisms, treatment recommendations and future research. World J Diabetes. 2015;6(13):1246–58.

28. Murata M, Adachi H, Oshima S, Kurabayashi M. Glucose fluctuation and the resultant endothelial injury are correlated with pancreatic β cell dysfunction in patients with coronary artery disease. Diabetes Res Clin Pract. 2017.

29. Siracuse JJ, Chaikof EL. The Pathogenesis of Diabetic Atherosclerosis. 2012;13–27.

30. Holland WL, Knotts T a, Chavez J a, Wang L-P, Hoehn KL, Summers S a. Lipid mediators of insulin resistance. Nutr Rev. 2007;65(6 Pt 2):S39–46.

31. Vaag A, Lund SS. Non-obese patients with type 2 diabetes and prediabetic subjects: distinct phenotypes requiring special diabetes treatment and (or) prevention? Appl Physiol Nutr Metab. 2007;32(5):912–20.

32. Muñoz-Garach A, Cornejo-Pareja I, Tinahones FJ. Does metabolically healthy obesity exist? Nutrients. 2016;8(6):1–10.

33. Lemoine AY, Ledoux S, Larger E. Adipose tissue angiogenesis in obesity. Thromb Haemost. 2013;110(4):661–9.

34. Marzolla V, Armani A, Zennaro MC, Cinti F, Mammi C, Fabbri A, et al. The role of the mineralocorticoid receptor in adipocyte biology and fat metabolism. Mol Cell Endocrinol. 2012;350(2):281–8.

35. Molica F, Morel S, Kwak BR, Rohner-Jeanrenaud F, Steffens S. Adipokines at the crossroad between obesity and cardiovascular disease. Thromb Haemost. 2015;113(3):553–66.

36. Bulcão C, Ferreira SRG, Giuffrida FMA, Ribeiro-Filho FF. The new adipose tissue and adipocytokines. Curr Diabetes Rev. 2006;2(1):19–28.

37. Scherer PE. Adipose tissue: From lipid storage compartment to endocrine organ. Diabetes. 2006;55(6):1537–45.

38. Choe SS, Huh JY, Hwang IJ, Kim JI, Kim JB. Adipose Tissue Remodeling: Its Role in Energy Metabolism and Metabolic Disorders. Front Endocrinol. 2016;7:30.

39. Park A, Kim WK, Bae K-H. Distinction of white, beige and brown adipocytes derived from mesenchymal stem cells. World J Stem Cells. 2014;6(1):33–42.

40. Saely CH, Geiger K, Drexel H. Brown versus white adipose tissue: A mini-review. Gerontology. 2011;58(1):15–23.

41. Cedikova M, Kripnerová M, Dvorakova J, Pitule P, Grundmanova M, Babuska V, et al. Mitochondria in White, Brown, and Beige Adipocytes. Stem Cells Int. 2016.

42. Cannon B, Nedergaard J. Brown adipose tissue: function and physiological significance. Physiol Rev. 2004;84(1):277–359.

43. Peirce V, Carobbio S, Vidal-Puig A. The different shades of fat. Nature. 2014;510(7503):76–83.

44. Rosen, Even D. and Spiegelman BM. Adipocytes as regulators of energy balance and glucose homeostasis. 2006;

45. Corvera S, Gealekman O. Adipose tissue angiogenesis: Impact on obesity and type-2 diabetes. Biochim Biophys Acta - Mol Basis Dis. 2014;1842(3):463–72.

46. Leonardini A, Laviola L, Perrini S, Natalicchio A, Giorgino F. Cross-Talk between PPARγ and Insulin Signaling and Modulation of Insulin Sensitivity. PPAR Res. 2009;3;2009:818945.

47. Ruderman NB, Carling D, Prentki M, Cacicedo JM. AMPK, insulin resistance, and the metabolic syndrome. J Clin Invest. 2013;123(7):2764–72.

48. Kusminski CM, McTernan PG, Kumar S. Role of resistin in obesity, insulin

resistance and Type II diabetes. Clin Sci. 2005;109(3):243–56.

49. Trayhurn P, Beattie JH. Physiological role of adipose tissue: white adipose tissue as an endocrine and secretory organ. Proc Nutr Soc. 2001;60(3):329–39.

50. Bays HE, González-Campoy JM, Bray GA, Kitabchi AE, Bergman DA, Schorr AB, et al. Pathogenic potential of adipose tissue and metabolic consequences of adipocyte hypertrophy and increased visceral adiposity. Expert Rev Cardiovasc Ther. 2008;6(3):343–68.

51. Zmijewski JW, Banerjee S, Bae H, Friggeri A, Lazarowski ER, Abraham E. Exposure to hydrogen peroxide induces oxidation and activation of AMP-activated protein kinase. J Biol Chem. 2010;285(43):33154–64.

52. Iacobellis G. Local and systemic effects of the multifaceted epicardial adipose tissue depot. Nat Rev Endocrinol. 2015;11(6):363–71.

53. Iacobellis G, Corradi D, Sharma AM. Epicardial adipose tissue: anatomic, biomolecular and clinical relationships with the heart. Nat Clin Pract Cardiovasc Med. 2005;2(10):536–43.

54. Marchington JM, Mattacks CA PC. Adipose tissue in the mammalian heart and pericardium; structure, fetal development and biochemical properties. Comp Biochem Physiol. 1989;94(2):225–32.

55. Wronkowitz N, Romacho T, Sell H, Eckel J. Adipose tissue dysfunction and inflammation in cardiovascular disease. Front Horm Res. 2014;43:79–92.

56. Iozzo P. Myocardial, perivascular,and epicardial fat. Diabetes Care. 2011;34(SUPPL. 2).

57. Iacobellis G. Epicardial and Pericardial Fat: Close, but Very Different. Obesity. 2009;17(4):625–625.

58. Cherian S, Lopaschuk GD, Carvalho E. Cellular cross-talk between epicardial adipose tissue and myocardium in relation to the pathogenesis of cardiovascular disease. Am J Physiol Endocrinol Metab. 2012;303(8):E937-49.

59. Fitzgibbons TP, Czech MP. Epicardial and perivascular adipose tissues and their influence on cardiovascular disease: basic mechanisms and clinical associations. J Am Heart Assoc. 2014;3(2):1–15.

60. Wu Y, Zhang A, Hamilton DJ, Deng T. Epicardial fat in the maintenance of cardiovascular health. 2017;(1):20–4.

61. Corradi D, Maestri R, Callegari S, Pastori P, Goldoni M, Luong TV, et al. The ventricular epicardial fat is related to the myocardial mass in normal, ischemic and hypertrophic hearts. Cardiovasc Pathol. 2004;13(6):313–6.

62. Iacobellis G. Epicardial fat: A new cardiovascular therapeutic target. Curr Opin Pharmacol. 2016;27:13–8.

63. Antonopoulos AS, Antoniades C. The role of epicardial adipose tissue in cardiac biology: classic concepts and emerging roles. J Physiol. 2017;00:1–11.

64. Chechi K, Blanchard PG, Mathieu P, Deshaies Y, Richard D. Brown fat like gene expression in the epicardial fat depot correlates with circulating HDL-cholesterol and triglycerides in patients with coronary artery disease. Int J Cardiol. 2013;167(5):2264–70.

65. Sacks HS, Fain JN, Holman B, Cheema P, Chary A, Parks F, et al. Uncoupling protein-1 and related messenger ribonucleic acids in human epicardial and other adipose tissues: Epicardial fat functioning as brown fat. J Clin Endocrinol Metab. 2009;94(9):3611–5.

66. Gaborit B, Venteclef N, Ancel P, Pelloux V, Gariboldi V, Leprince P, et al. Human epicardial adipose tissue has a specific transcriptomic signature depending on its anatomical peri-atrial, peri-ventricular, or peri-coronary location. Cardiovasc Res. 2015;108(1):62–73.

67. Antonopoulos AS, Margaritis M, Coutinho P, Digby J, Patel R, Psarros C, et al. Reciprocal effects of systemic inflammation and brain natriuretic peptide on adiponectin biosynthesis in adipose tissue of patients with ischemic heart disease. Arterioscler Thromb Vasc Biol. 2014;34(9):2151–9.

68. Baker AR, Silva NF da, Quinn DW, Harte AL, Pagano D, Bonser RS, et al. Human epicardial adipose tissue expresses a pathogenic profile of adipocytokines in patients with cardiovascular disease. Cardiovasc Diabetol. 2006;5:1.

69. Turer AT, Scherer PE. Adiponectin: Mechanistic insights and clinical implications. Diabetologia. 2012;55(9):2319–26.

70. Venteclef N, Guglielmi V, Balse E, Gaborit B, Cotillard A, Atassi F, et al. Human epicardial adipose tissue induces fibrosis of the atrial myocardium through the secretion of adipo-fibrokines. Eur Heart J. 2015;36(13):795–805.

71. Pérez-Belmonte LM, Moreno-Santos I, Cabrera-Bueno F, Sánchez-Espín G, Castellano D, Such M, et al. Expression of sterol regulatory element-binding proteins in epicardial adipose tissue in patients with coronary artery disease and diabetes mellitus: Preliminary study. Int J Med Sci. 2017;14(3):268–74.

72. Noyes AM. Cardiac adipose tissue and its relationship to diabetes mellitus and cardiovascular disease. World J Diabetes. 2014;5(6):868.

73. Ouchi N, Parker JL, Lugus JJ, Walsh K. Adipokines in inflammation and metabolic disease. Vol. 11, Nature reviews. Immunology. 2011.p. 85–97.

74. Antonopoulos AS, Margaritis M, Verheule S, Recalde A, Sanna F, Herdman L, et al. Mutual regulation of epicardial adipose tissue and myocardial redox state by PPAR-γ/adiponectin signalling. Circ Res. 2016;118(5):842–55.

75. Fang X, Palanivel R, Cresser J, Schram K, Ganguly R, Thong FSL, et al. An APPL1-AMPK signaling axis mediates beneficial metabolic effects of adiponectin in the

heart. Vol. 299, American Journal of Physiology - Endocrinology and Metabolism. Bethesda, MD; 2010. p. E721-9.

76. Pezeshkian M, Noori M, Najjarpour-Jabbari H, Abolfathi A, Darabi M, Darabi M, et al. Fatty acid composition of epicardial and subcutaneous human adipose tissue. Metab Syndr Relat Disord. 2009;7(2):125–31.

77. Gastaldelli A, Morales MA, Marraccini P, Sicari R. The role of cardiac fat in insulin resistance. Curr Opin Clin Nutr Metab Care. 2012;15(6):523–8.

78. Blumensatt M, Fahlbusch P, Hilgers R, Bekaert M, Herzfeld de Wiza D, Akhyari P, et al. Secretory products from epicardial adipose tissue from patients with type 2 diabetes impair mitochondrial B-oxidation in cardiomyocytes via activation of the cardiac renin-angiotensin system and induction of miR-208a. Basic Res Cardiol. 2017;112(1):1–13.

79. Shimabukuro M, Hirata Y, Tabata M, Dagvasumberel M, Sato H, Kurobe H, et al. Epicardial adipose tissue volume and adipocytokine imbalance are strongly linked to human coronary atherosclerosis. Arterioscler Thromb Vasc Biol. 2013;33(5):1077–84.

80. Burgeiro A, Fuhrmann A, Cherian S, Espinoza D, Jarak I, Carvalho RA, et al. Glucose uptake and lipid metabolism are impaired in epicardial adipose tissue from heart failure patients with or without diabetes. Am J Physiol - Endocrinol Metab. 2016;310(7):E550–64.

81. Iacobellis G, Barbaro G. The double role of epicardial adipose tissue as pro- and anti-inflammatory organ. Horm Metab Res. 2008;40(7):442–5.

82. Mazurek T, Zhang L, Zalewski A, Mannion JD, Diehl JT, Arafat H, et al. Human Epicardial Adipose Tissue Is a Source of Inflammatory Mediators. Circulation. 2003;108(20):2460–6.

83. Hirata Y, Tabata M, Kurobe H, Motoki T, Akaike M, Nishio C, et al. Coronary atherosclerosis is associated with macrophage polarization in epicardial adipose tissue. J Am Coll Cardiol. 2011;58(3):248–55.

84. Cancello R, Henegar C, Viguerie N, Taleb S, Poitou C, Rouault C, et al. Reduction of macrophage infiltration and chemoattractant gene expression changes in white adipose tissue of morbidly obese subjects after surgery-induced weight loss. Diabetes. 2005;54(8):2277–86.

85. Greulich S, Maxhera B, Vandenplas G, De Wiza DH, Smiris K, Mueller H, et al. Secretory products from epicardial adipose tissue of patients with type 2 diabetes mellitus induce cardiomyocyte dysfunction. Circulation. 2012;126(19):2324–34.

86. Greulich S, de Wiza DH, Preilowski S, Ding Z, Mueller H, Langin D, et al. Secretory products of guinea pig epicardial fat induce insulin resistance and impair primary adult rat cardiomyocyte function. J Cell Mol Med. 2011;15(11):2399–410.

87. Jiang D-S, Zeng H-L, Li R, Huo B, Su Y-S, Fang J, et al. Aberrant Epicardial Adipose

Tissue Extracellular Matrix Remodeling in Patients with Severe Ischemic Cardiomyopathy: Insight from Comparative Quantitative Proteomics. Sci Rep. 2017;7:43787.

88. Bachar GN, Dicker D, Kornowski R, Atar E. Epicardial adipose tissue as a predictor of coronary artery disease in asymptomatic subjects. Am J Cardiol. 2012;110(4):534–8.

89. Iwasaki K, Matsumoto T, Aono H, Furukawa H, Samukawa M. Relationship between epicardial fat measured by 64-multidetector computed tomography and coronary artery disease. Clin Cardiol. 2011;34(3):166–71.

90. Lima-Martinez MM, Paoli M, Rodney M, Balladares N, Contreras M, Marco LD, et al. Effect of sitagliptin on epicardial fat thickness in subjects with type 2 diabetes and obesity: a pilot study. Endocrine. 2016;51(3):448–55.

91. Iacobellis G, Camarena V, Sant DW, Wang G, Res HM. Human Epicardial Fat Expresses Glucagon-Like Peptide 1 and 2 Receptors Genes Authors. 2017;

92. Iacobellis G, Mohseni M, Bianco SD, Banga PK. Liraglutide causes large and rapid epicardial fat reduction. Obesity. 2017;25(2):311–6.

93. Leney SE, Tavaré JM. The molecular basis of insulin-stimulated glucose uptake: Signalling, trafficking and potential drug targets. J Endocrinol. 2009;203(1):1–18.

94. De Pauw A, Tejerina S, Raes M, Keijer J, Arnould T. Mitochondrial (dys)function in adipocyte (de)differentiation and systemic metabolic alterations. Am J Pathol. 2009;175(3):927–39.

95. Logan DC. The mitochondrial compartment. J Exp Bot. 2006;57(6):1225–43.

96. Zhang Y, Zeng X, Jin S. Autophagy in adipose tissue biology. Pharmacol Res. 2012;66(6):505–12.

97. Wang CH, Wang CC, Wei YH. Mitochondrial dysfunction in insulin insensitivity: Implication of mitochondrial role in type 2 diabetes. Ann N Y Acad Sci. 2010;1201:157–65.

98. Zeviani M, Di Donato S. Mitochondrial disorders. Brain. 2004;127(10):2153–72.

99. Benard G, Faustin B, Passerieux E, Galinier A, Rocher C, Bellance N, et al. Physiological diversity of mitochondrial oxidative phosphorylation. Am J Physiol Cell Physiol. 2006;291(6):C1172–82.

100. Schägger H, Pfeiffer K. Supercomplexes in the respiratory chains of yeast and mammalian mitochondria. EMBO J. 2000 Apr 17;19(8):1777–83.

101. Wong HS, Dighe PA, Mezera V, Monternier PA, Brand MD. Production of superoxide and hydrogen peroxide from specific mitochondrial sites under different bioenergetic conditions. J Biol Chem. 2017;292(41):16804–9.

102. J A Kim, Y Wei JRS. Role of Mitochondrial Dysfunction in Insulin Resistance.

2010;102(4):401–14.

103. Bhat AH, Dar KB, Anees S, Zargar MA, Masood A, Sofi MA, et al. Oxidative stress, mitochondrial dysfunction and neurodegenerative diseases; a mechanistic insight. Biomed Pharmacother. 2015;74:101–10.

104. Gnaiger E, Kuznetsov A V. Mitochondrial respiration at low levels of oxygen and cytochrome c. Biochem Soc Trans. 2002;30(2):252–8.

105. Williams GSB, Boyman L, Chikando AC, Khairallah RJ, Lederer WJ. Mitochondrial calcium uptake. Proc Natl Acad Sci U S A. 2013;110(26):10479–86.

106. Boudina S, Graham TE. Mitochondrial function/dysfunction in white adipose tissue. Exp Physiol. 2014;99(9):1168–78.

107. Czabotar PE, Lessene G, Strasser A, Adams JM. Control of apoptosis by the BCL-2 protein family: implications for physiology and therapy. Nat Rev Mol Cell Biol. 2014 Jan;15(1):49–63.

108. Starkov A. The role of Mitochondria in Reactive Oxygen Species Metabolism and Signaling. 2008;351(2):37–52.

109. Wilson-fritch L, Burkart A, Bell G, Leszyk J, Nicoloro S, Czech M, et al. Mitochondrial Biogenesis and Remodeling during Adipogenesis and in Response to the Insulin Sensitizer Rosiglitazone Mitochondrial Biogenesis and Remodeling during Adipogenesis and in Response to the Insulin Sensitizer Rosiglitazone. Mol Cell Biol. 2003;23(3):1085–94.

110. Gregoire FM, Smas CM, Sul HS. Understanding adipocyte differentiation. Physiol Rev. 1998;78(3):783–809.

111. Tormos K. Mitochondrial complex III ROS regulate adipocyte differentiation. Cell Metab. 2011;76:211–20.

112. Rosen ED, Sarraf P, Troy AE, Bradwin G, Moore K, Milstone DS, et al. PPARγ is required for the differentiation of adipose tissue in vivo and in vitro. Mol Cell. 1999;4(4):611–7.

113. Liu D, Lin Y, Kang T, Huang B, Xu W, Garcia-Barrio M, et al. Mitochondrial dysfunction and adipogenic reduction by prohibitin silencing in 3T3-L1 cells. PLoS One. 2012;7(3):1–10.

114. Puigserver P, Spiegelman BM. Peroxisome proliferator-activated receptor-γ coactivator 1α (PGC-1α): Transcriptional coactivator and metabolic regulator. Endocr Rev. 2003;24(1):78–90.

115. Kajimoto K, Terada H, Baba Y, Shinohara Y. Essential role of citrate export from mitochondria at early differentiation stage of 3T3-L1 cells for their effective differentiation into fat cells, as revealed by studies using specific inhibitors of mitochondrial di- and tricarboxylate carriers. Mol Genet Metab. 2005;85(1):46–53.

116. Li P, Zhu Z, Lu Y, Granneman JG, James G. Metabolic and cellular plasticity in white adipose tissue II : role of peroxisome proliferator-activated receptor-a. Am J Physiol Endocrinol Metab. 2005;289:E617–26.

117. Sugden MC, Holness MJ. Mechanisms underlying regulation of the expression and activities of the mammalian pyruvate dehydrogenase kinases. Arch Physiol Biochem. 2006;112(3):139–49.

118. Fassina G, Badetti R, Visco L, Dorigo P. Effect of Oxidative-Phosphorylation Inhibitors on Cyclic Adenosine Monophosphate Synthesis in Rat Adipose-Tissue. Biochem Pharmacol. 1972;21(11):1633-.

119. Fassina G. Equilibrium between metabolic pathways producing energy: a key factor in tegulating lipolysis. Pharmacol Res Commun. 1974;6(1).

120. Nascimento CMO Do, Ribeiro EB, Oyama LM. Metabolism and secretory function of white adipose tissue: effect of dietary fat. An Acad Bras Cienc. 2009;81(3):453–66.

121. Busiello RA, Savarese S, Lombardi A. Mitochondrial uncoupling proteins and energy metabolism. Front Physiol. 2015;6:36.

122. Divakaruni AS, Brand MD. The Regulation and Physiology of Mitochondrial Proton Leak. Physiology. 2011;26(3):192–205.

123. Lowell BB, Spiegelman BM. Towards a molecular understanding of adaptive thermogenesis. Nature. 2000;404:652.

124. Shan T, Liang X, Bi P, Zhang P, Liu W, Kuang S. Distinct populations of adipogenic and myogenic Myf5-lineage progenitors in white adipose tissues. J Lipid Res. 2013;54(8):2214–24.

125. Xiwei Zheng, Cong Bi, Marissa Brooks and DSH. Adipocytes arise from multiple lineages that are heterogeneously and dynamically distributed Joan. Anal Chem. 2015;25(4):368–79.

126. Sacks HS, Fain JN, Bahouth SW, Ojha S, Frontini A, Budge H, et al. Adult epicardial fat exhibits beige features. J Clin Endocrinol Metab. 2013;98(9):1448–55.

127. Lanner JT, Katz A, Tavi P, Sandström ME, Zhang SJ, Wretman C, et al. The role of Ca2+ influx for insulin-mediated glucose uptake in skeletal muscle. Diabetes. 2006;55(7):2077–83.

128. Lanner JT, Bruton JD, Katz A, Westerblad H. Ca2+ and insulin-mediated glucose uptake. Curr Opin Pharmacol. 2008;8(3):339–45.

129. Kriszt R, Arai S, Itoh H, Lee MH, Goralczyk AG, Ang XM, et al. Optical visualisation of thermogenesis in stimulated single-cell brown adipocytes. Sci Rep. 2017;7(1):1383.

130. Kontani Y, Wang Y, Kimura K, Inokuma KI, Saito M, Suzuki-Miura T, et al. UCP1 deficiency increases susceptibility to diet-induced obesity with age. Aging Cell.

2005;4(3):147–55.

131. Patel P, Abate N. Role of subcutaneous adipose tissue in the pathogenesis of insulin resistance. J Obes. 2013.

132. Frayn K. Adipose tissue as a buffer for daily lipid flux. Diabetologia. 2002;45(9):1201–10.

133. Vidal-Puig AJ, Considine R V, Jimenez-Liñan M, Werman A, Pories WJ, Caro JF, et al. Peroxisome proliferator-activated receptor gene expression in human tissues. Effects of obesity, weight loss, and regulation by insulin and glucocorticoids. J Clin Invest. 1997;99(10):2416–22.

134. Thermo Fisher Scienctific. Protein assay technical handbook Tools and reagents for improved quantitation of total or specific proteins. 2017;

135. Gnaiger E. The Oxygraph for High-Resolution Respirometry. Mitochondr Physiol Netw. 2007;6.1:1–19.

136. Doerrier C, Garcia-Souza LF, Krumschnabel G, Wohlfarter Y, Mészáros AT, Gnaiger E. High-resolution fluorespirometry and oxphos protocols for human cells, permeabilized fibers from small biopsies of muscle, and isolated mitochondria. Methods Mol Biol. 2018;1782.

137. Hansen M, Lund MT, Gregers E, Kraunsøe R, Van Hall G, Helge JW, et al. Adipose tissue mitochondrial respiration and lipolysis before and after a weight loss by diet and RYGB. Obesity. 2015;23(10):2022–9.

138. Woyda-ploszczyca AM, Jarmuszkiewicz W. Different Effects of Guanine Nucleotides (GDP and GTP) on Protein-Mediated Mitochondrial Proton Leak. 2014;9:e98969.

139. Iacobellis G, Corradi D, Sharma AM. Epicardial adipose tissue: anatomic, biomolecular and clinical relationships with the heart. Nat Clin Pract Cardiovasc Med. 2005;2(10):536–43.

140. Bambace C, Telesca M, Zoico E, Sepe A, Olioso D, Rossi A, et al. Adiponectin gene expression and adipocyte diameter: A comparison between epicardial and subcutaneous adipose tissue in men. Cardiovasc Pathol. 2011;20(5):e153–6.

141. Lu M, Wan M, Leavens KF, Chu Q, Monks BR, Fernandez S, et al. Insulin regulates liver metabolism in vivo in the absence of hepatic Akt and Foxo1. Nat Med. 2012;18:388.

142. Shearin AL, Monks BR, Seale P, Birnbaum MJ. Lack of AKT in adipocytes causes severe lipodystrophy. Mol Metab. 2016;5(7):472–9.

143. Cho H, Mu J, Kim JK, Thorvaldsen JL, Chu Q, Crenshaw EB, et al. Insulin Resistance and a Diabetes Mellitus-Like Syndrome in Mice Lacking the Protein Kinase Akt2 (PKBβ). Science (80-). 2001;292(5522):1728 LP-1731.

144. García-Casarrubios E, de Moura C, Arroba AI, Pescador N, Calderon-Dominguez

M, Garcia L, et al. Rapamycin negatively impacts insulin signaling, glucose uptake and uncoupling protein-1 in brown adipocytes. Biochim Biophys Acta - Mol Cell Biol Lipids. 2016;1861(12):1929–41.

145. Bost F, Aouadi M, Caron L, Binétruy B. The role of MAPKs in adipocyte differentiation and obesity. Biochimie. 2005;87(1 SPEC. ISS.):51–6.

146. Obata T, Brown GE, Yaffe MB. MAP kinase pathways activated by stress: The p38 MAPK pathway. Crit Care Med. 2000;28(4).

147. Johnson GL, Nakamura K. The c-jun kinase/stress-activated pathway: Regulation, function and role in human disease. Biochim Biophys Acta - Mol Cell Res. 2007;1773(8):1341–8.

148. Burgeiro A, Fonseca AC, Espinoza D, Carvalho L, Lourenço N, Antunes M, et al. Proteostasis in epicardial versus subcutaneous adipose tissue in heart failure subjects with and without diabetes. Biochim Biophys Acta - Mol Basis Dis. 2018;1864(6, Part A):2183–98.

149. Maixner N, Bechor S, Vershinin Z, Pecht T, Goldstein N, Haim Y, et al. Transcriptional Dysregulation of Adipose Tissue Autophagy in Obesity. Physiology. 2016;31(4):270–82.

150. Wakil SJ. Fatty acid synthase, a proficient multifunctional enzyme. Biochemistry. 1989;28(11):4523–30.

151. Werner JC, Sicard RE, Schuler HG. Palmitate oxidation by isolated working fetal and newborn pig hearts. Am J Physiol Metab. 1989;256(2):E315–21.

152. Fonseca AC, Burgeiro A, Dias C, Baldeiras I, Cunha-Oliveira T, Lourenço N, et al. Increased bioenergetics and decreased oxidative stress markers is observed in Epicardial compared to Subcutaneous fat in heart failure subjects. Manuscr Prep.

153. Larsen S, Nielsen J, Hansen CN, Nielsen LB, Wibrand F, Stride N, et al. Biomarkers of mitochondrial content in skeletal muscle of healthy young human subjects. J Physiol. 2012;590(14):3349–60.

154. Sharma M, Garber A, Farmer J. Role of Insulin Signaling in Maintaining Energy Homeostasis. Endocr Pract. 2008;14(3):373–80.

155. Hernandez R, Teruel T, Lorenzo M. Akt mediates insulin induction of glucose uptake and up-regulation of GLUT4 gene expression in brown adipocytes. FEBS Lett. 2001;494(3):225–31.

156. Kotzka J, Lehr S, Roth G, Avci H, Knebel B, Muller-Wieland D. Insulin-activated Erk-mitogen-activated protein kinases phosphorylate sterol regulatory element-binding protein-2 at serine residues 432 and 455 in vivo. J Biol Chem. 2004;279(21):22404–11.

157. Rydén M, Arvidsson E, Blomqvist L, Perbeck L, Dicker A, Arner P. Targets for TNF-α-induced lipolysis in human adipocytes. Biochem Biophys Res Commun.

2004;318(1):168–75.

158. Greenberg AS, Shen WJ, Muliro K, Patel S, Souza SC, Roth RA, et al. Stimulation of Lipolysis and Hormone-sensitive Lipase via the Extracellular Signal-regulated Kinase Pathway. J Biol Chem. 2001;276(48):45456–61.

159. Boudina S, Graham TE. Mitochondrial function/dysfunction in white adipose tissue. Exp Physiol. 2014 Aug 11;99(9):1168–78.

160. Calderon-Dominguez M, Alcalá M, Sebastián D, Zorzano A, Viana M, Serra D, et al. Brown Adipose Tissue Bioenergetics: A New Methodological Approach. Adv Sci. 2017;4(4).

161. Fedorenko A, Lishko P V., Kirichok Y. Mechanism of fatty-acid-dependent UCP1 uncoupling in brown fat mitochondria. Cell. 2012;151(2):400–13.

162. Divakaruni AS, Humphrey DM, Brand MD. Fatty acids change the conformation of uncoupling protein 1 (UCP1). J Biol Chem. 2012;287(44):36845–53.

163. Buck E, Zügel M, Schumann U, Merz T, Gumpp AM, Witting A, et al. High-resolution respirometry of fine-needle muscle biopsies in pre-manifest Huntington's disease expansion mutation carriers shows normal mitochondrial respiratory function. PLoS One. 2017;12(4):1–21.

164. Chicco AJ, Le CH, Schlater A, Nguyen A, Kaye S, Beals JW, et al. High fatty acid oxidation capacity and phosphorylation control despite elevated leak and reduced respiratory capacity in northern elephant seal muscle mitochondria. J Exp Biol. 2014;217:2947–55.

165. Vijgen GHEJ, Sparks LM, Bouvy ND, Schaart G, Hoeks J, van Marken Lichtenbelt WD, et al. Increased Oxygen Consumption in Human Adipose Tissue From the "Brown Adipose Tissue" Region. J Clin Endocrinol Metab. 2013;98(7):E1230–4.

166. Phielix E, Schrauwen-hinderling VB, Mensink M, Lenaers E, Meex R, Hoeks J, et al. Lower intrinsic ADP stimulated mitochondrial respirationin underlies in vivo mitochondrial dysfunction in muscle of male type 2 diabetic patients. Diabetes. 2008;57:2943–9.

167. Forouhi NG, Koulman A, Sharp SJ, Imamura F, Kröger J, Schulze MB, et al. Differences in the prospective association between individual plasma phospholipid saturated fatty acids and incident type 2 diabetes: The EPIC-InterAct case-cohort study. Lancet Diabetes Endocrinol. 2014;2(10):810–8.

168. Dirkx E, Schwenk RW, Glatz JFC, Luiken JJFP, van Eys GJJM. High fat diet induced diabetic cardiomyopathy. Prostaglandins, Leukot Essent Fat Acids. 2011;85(5):219–25.